WATER-RESOURCES ENGINEERING

Fourth Edition

DAVID A. CHIN

WATER-RESOURCES ENGINEERING

Fourth Edition

David A. Chin, Ph.D., P.E., BCEE
Professor of Civil and Environmental Engineering
University of Miami

Pearson

Library of Congress Cataloging-in-Publication Data

Names: Chin, David A., author. | Pearson (Firm)
Title: Water-resources engineering / David A. Chin.
Other titles: Water resources engineering
Description: Fourth Edition. | Hoboken, New Jersey : Pearson, 2020. | Third edition published in 2013. | Includes bibliographical references and index.
Identifiers: LCCN 2019044296 | ISBN 9780135357705 (Paperback)
Subjects: LCSH: Hydraulics. | Hydrology. | Waterworks. | Water resources development.
Classification: LCC TC160 .C52 2020 | DDC 627–dc23
LC record available at https://lccn.loc.gov/2019044296

ScoutAutomatedPrintCode

Access Card
ISBN 10: 0-13-535770-5
ISBN 13: 978-0-13-535770-5

Instructor's Review Copy
ISBN 10: 0-13-670710-6
ISBN 13: 978-0-13-670710-3

Rental Edition
ISBN 10: 0-13-668151-4
ISBN 13: 978-0-13-668151-9

Loose-Leaf Edition
ISBN 10: 0-13-561742-1
ISBN 13: 978-0-13-561742-7

Pearson

Contents

Preface

Water-resources engineers design systems to control the quantity, quality, timing, and distribution of water to support human habitation and the needs of the environment. Water-supply and flood-control systems are commonly regarded as essential infrastructure for developed areas, and as such water-resources engineering is a core specialty area in civil engineering. Water-resources engineering is also a specialty area in environmental engineering, particularly with regard to the design of water-supply systems, wastewater-collection systems, and water-quality control in natural systems.

Overview of book contents. The technical and scientific bases for most water-resources applications are in the areas of hydraulics and hydrology, and this text covers these areas with depth and rigor. The fundamentals of closed-conduit flow, open-channel flow, surface-water hydrology, groundwater hydrology, and water-resources planning and management are all covered in detail. Applications of these fundamentals include the design of water-distribution systems, hydraulic structures, sanitary-sewer systems, stormwater-management systems, and water-supply wellfields. The design protocols for these systems are guided by the relevant ASCE, WEF, and AWWA manuals of practice, as well as USFHWA design guidelines for urban and transportation-related drainage structures, and USACE design guidelines for hydraulic structures. The topics covered in this book constitute the technical background expected of water-resources engineers. This text is appropriate for undergraduate and first-year graduate courses in hydraulics, hydrology, and water-resources engineering. Practitioners will also find the material in this book to be a useful reference on appropriate design protocols.

Organization of book. The book has been organized in such a way as to sequentially cover the theory and design applications in each of the key areas of water-resources engineering. The theory of flow in closed conduits is covered in Chapter 2, including applications of the continuity, momentum, and energy equations to flow in closed conduits, calculation of water-hammer pressures, flows in pipe networks, affinity laws for pumps, pump performance curves, and procedures for pump selection and assessing the performance of multi-pump systems. The design of public water-supply systems and building water-supply systems are covered in Chapter 3, which includes the estimation of water demand, design of pipelines, pipeline appurtenances, service reservoirs, performance criteria for water-distribution systems, and several practical design examples. The theory of flow in open channels is covered in Chapter 4, which includes applications of the continuity, momentum, and energy equations to flow in open channels, and computation of water-surface profiles. The design of drainage channels is covered in Chapter 5, which includes the application of design standards for determining the appropriate channel dimensions for various channel linings, including vegetative and nonvegetative linings. The design of sanitary-sewer systems is covered in Chapter 6, which includes design approaches for estimating the quantity of wastewater to be handled by sewers; sizing sewer pipes based on self-cleansing and capacity using the ASCE-recommended tractive-force method; and the performance of manholes, force mains, pump stations, and hydrogen-sulfide control systems are also covered. Design of the most widely used hydraulic structures is covered in Chapter 7, which includes the design of culverts, gates, weirs, spillways, stilling basins, dams, and hydropower facilities. This chapter is particularly important since most water-resources projects rely on the performance of hydraulic structures to achieve their objectives. The bases for the design of water-resources systems are typically rainfall and/or surface runoff, which are random variables that must generally be specified probabilistically. Applications of probability and statistics in water-resources engineering are covered in detail in Chapter 8, with particular emphasis on the analysis of hydrologic data and uncertainty analysis in predicting hydrologic variables. The fundamentals of surface-water hydrology are covered in Chapters 9 and 10. These chapters cover the statistical characterization of rainfall for design applications, methodologies for estimating peak runoff rates and runoff hydrographs, methodologies for routing runoff hydrographs through detention basins, and methods for estimating the quality of surface runoff. The design of stormwater-collection systems is covered in Chapter 11, including the design of stormwater inlets and storm sewers. Stormwater-management systems are designed to treat stormwater prior to discharge into receiving waters, and the design of these systems is covered in Chapter 12. Several state-of-the-art design examples for the most commonly used stormwater-control measures, including green infrastructure, are provided. Coverage includes the design of infiltration basins, swales, filter strips, bioretention systems, green roofs, permeable pavements, exfiltration trenches, and drainage wells. The estimation of evapotranspiration, which is usually the dominant component of seasonal and annual water budgets in arid areas and a core component in the design of irrigation systems, is covered in Chapter 13. The fundamentals of groundwater hydrology are covered in Chapters 14 and 15, including an exposition on Darcy's law, derivation of the general groundwater flow equation, practical solutions to the groundwater flow equation, and methods to assess and control saltwater intrusion in coastal aquifers. Applications of groundwater hydrology to the design of wellfields, the delineation of wellhead protection areas, and the design of wells are all covered. Water-resources planning typically includes identifying alternatives and ranking the alternatives based on specified criteria. Chapter 17 covers the conventional approaches for identifying and ranking alternatives and the bases for the economic evaluation of these alternatives.

Summary. In summary, this book provides an in-depth coverage of the subject areas that are fundamental to the practice of water-resources engineering. A firm grasp of the material covered in this book along with complementary practical experience are the foundations on which water-resources engineering is practiced at the highest level. Throughout the entire textbook, equations contained within boxes represent derived equations that are particularly useful in engineering applications. In contrast, equations without boxes are typically intermediate equations within an analysis leading to a derived useful equation.

Philosophy. This book is a reflection of the author's belief that water-resources engineers must gain a firm understanding of the depth and breadth of the technical areas that are fundamental to their discipline, and by so doing will be more innovative, view water-resource systems holistically, and be technically prepared for a lifetime of learning. On the basis of this vision, the material contained in this book is presented mostly from first principles, is rigorous, is relevant to the practice of water-resources engineering, and is reinforced by detailed presentations of design applications.

What's New in the Fourth Edition

The fourth edition of this book contains much new and updated material relative to the previous edition. The most notable changes are as follows:

- Most figures have been enhanced to provide greater clarity in presentation and to facilitate understanding by the reader. The original versions of most figures are now available in color, and these color images can be presented using PowerPoint presentations that are available to instructors.
- The text presentation in the book has been significantly enhanced by using paragraph headings, which provides much greater clarity in the presented material.
- All design protocols reflect the latest design guidelines from the appropriate manuals of practice, and the material content reflects the latest advances as reported in professional journals.
- Many sections have been rewritten and updated, new sections have been added, and obsolete sections have been deleted. Notable changes are as follows:
  - A new section on pump-station design for sanitary sewers has been added.
  - The section on culvert design has been reorganized and rewritten to be consistent with the state-of-the-art practice.
  - The section relating to the estimation of intensity-duration-frequency (IDF) functions has been completely rewritten to reflect the emergence of Atlas 14 as the primary source of IDF functions in the United States.
  - The section relating to the design rainfall hyetographs has been updated to reflect the discontinuation of NRCS Type distributions in favor of more accurate local and regional synthetic rainfall distributions.
- The chapters on stormwater management (Chapter 12) and evapotranspiration (Chapter 13) have been almost completely updated in content. Chapter 12 now has increased coverage of removal capabilities of various stormwater control measures, including green infrastructure.
- More than 220 new end-of-chapter problems have been added, and these end-of-chapter problems have been segregated into groups that correspond to specific sections in the chapter.

This new edition reflects the state-of-the-art of water-resources engineering and is intended to provide the necessary competencies expected by the profession.

Instructor Resources

The following resources are available to instructors for download at www.pearsonhighered.com/irc. If you are in need of a login and password for this site, please contact your local Pearson representative.

- An Instructor Solution Manual contains solutions to the end-of-chapter problems.
- All figures from the text are available in PowerPoint presentations.

DAVID A. CHIN

Chapter 1

Introduction

1.1 Water-Resources Engineering

Water-resources engineering is an area of professional practice that includes the design of systems to control the quantity, quality, timing, and distribution of water to meet the needs of human habitation and the environment. Aside from the engineering and environmental aspects of water-resource systems, their feasibility from legal, economic, financial, political, and social viewpoints must generally be considered in the development process. The successful operation of an engineered system usually depends as much on nonengineering analyses (e.g., economic and social analyses) as on sound engineering design. Examples of water-resource systems include domestic, commercial, and industrial water supply, wastewater treatment, irrigation, drainage, flood control, salinity control, sediment control, pollution abatement, and hydropower-generation systems.

Cognate disciplines. The waters of the earth are found on land, in the oceans, and in the atmosphere, and the core science of water-resources engineering is *hydrology*, which deals with the occurrence, distribution, movement, and properties of water on Earth. Engineering hydrologists are primarily concerned with water on land and in the atmosphere, from its deposition as atmospheric precipitation to its inflow into the oceans and its evaporation into the atmosphere. Water-resources engineering is commonly regarded as a subdiscipline of civil engineering, and several other specialty areas are encompassed within the field of water-resources engineering. For example, the specialty area of groundwater hydrology is concerned with the occurrence and movement of water below the surface of the Earth; surface-water hydrology and climatology are concerned with the occurrence and movement of water above the surface of the Earth; hydrogeochemistry is concerned with the chemical changes in water that is in contact with earth materials; erosion, sedimentation, and geomorphology are concerned with the effects of sediment transport on landforms; and water policy, economics, and systems analyses are concerned with the political, economic, and environmental constraints in the design and operation of water-resource systems. The quantity and quality of water are inseparable issues in design, and the modern practice of water-resources engineering demands that practitioners be technically competent in understanding the physical processes that govern the movement of water, the chemical and biological processes that affect the quality of water, the economic and social considerations that must be taken into account, and the environmental impacts associated with the construction and operation of water-resource projects.

1.2 The Hydrologic Cycle

The *hydrologic cycle* is defined as the pathway of water as it moves in its various phases through the atmosphere, on and below the surface of the Earth, and back to the atmosphere. The movement of water in the hydrologic cycle is illustrated in Figure 1.1. A description of the hydrologic cycle can begin with the evaporation of water from the oceans, which is driven by energy from the sun. The evaporated water, in the form of water vapor, rises by convection, condenses in the atmosphere to form clouds, and precipitates onto land and ocean surfaces, predominantly as rain or snow. Rainfall on land surfaces is partially intercepted by surface vegetation, partially stored in surface depressions, partially infiltrated into the ground, and partially flows over land in natural and human-made drainage channels (e.g., rivers and aqueducts) that ultimately lead back to the ocean. Rainfall that is intercepted by surface vegetation is eventually evaporated into the atmosphere; water held in depression storage either evaporates or infiltrates into the ground; and water that infiltrates into the ground contributes to the recharge of groundwater, which either is utilized by plants, evaporates, is stored, or becomes subsurface flow that ultimately emerges as recharge to streams or directly to the ocean. Snowfall in mountainous areas typically accumulates in the winter and melts in the spring, thereby contributing to larger-than-average river flows during the spring. A typical example of the headwater of a stream being fed by snowmelt is shown in Figure 1.2. Since human-made systems are part of the hydrologic cycle, it is the responsibility of the water-resources engineer to ensure that systems constructed for water use and control are in harmony with the needs of the natural environment and the natural hydrologic cycle. In urban areas, the ground surface is typically much more impervious than in rural areas, and surface runoff in urban areas is mostly controlled by constructed drainage systems.

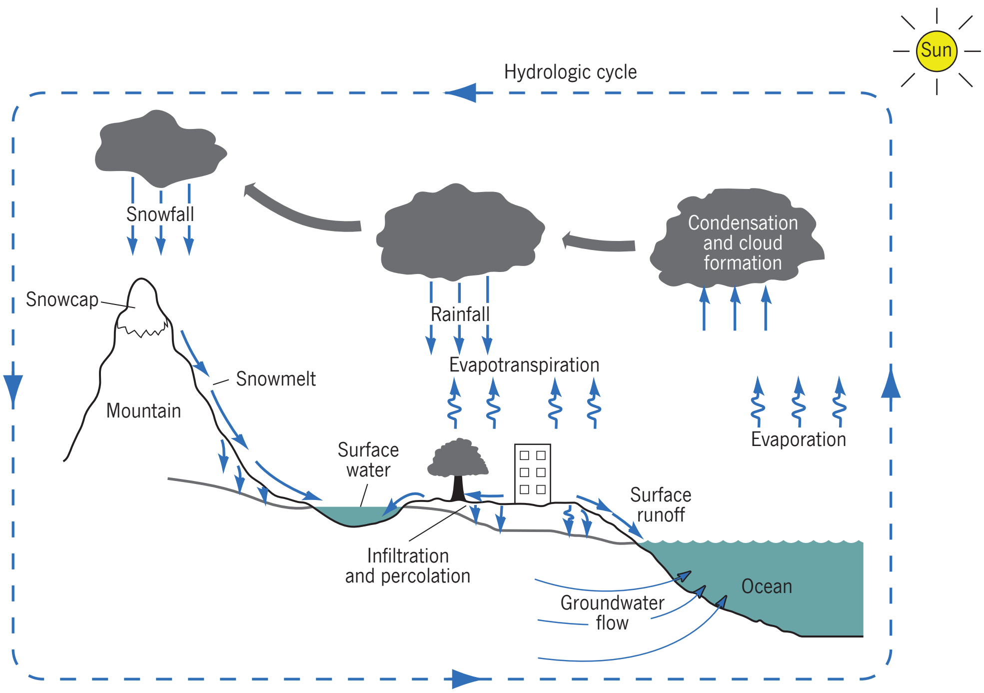

Figure 1.1: Hydrologic cycle

Figure 1.2: Snowmelt contribution to stream flow

Historical note: Up until the latter half of the seventeenth century, the nature of the hydrologic cycle was still in dispute, and the hypothesis that springs and rivers were recharged by percolation from the oceans back to the land remained a viable hypothesis. The modern concept of the hydrologic cycle has been generally accepted since Mariotte (1686) published calculations showing that rainfall in the Seine River basin was more than sufficient to account for flow in the Seine River.

Surface water and groundwater. Water above the land surface (in liquid form) is called *surface water*, and water below the land surface is called *groundwater*. Surface waters and groundwaters in urban areas tend to be significantly influenced by the water-supply and wastewater removal systems that are an integral part of the urban landscape. Governmental regulations are typically developed to control the development, design, and operation of surface-water and groundwater systems in urban areas.

Water quality. The quality of water varies considerably as it moves through the hydrologic cycle, with contamination potentially resulting from several sources. Classes of contaminants commonly found in water, along with some examples, are listed in Table 1.1. The effects of the quantity and quality of water on the health of terrestrial ecosystems, and the value of these ecosystems in the hydrologic cycle, are often overlooked. For example, the modification of free-flowing rivers for energy or water supply, and the drainage of wetlands, can have a variety of adverse effects on aquatic ecosystems, including losses in species diversity, floodplain fertility, and biofiltration capability. Also, excessive withdrawals of groundwater in coastal areas can cause saltwater intrusion, and hence deterioration of subsurface water quality.

Occurrence and distribution of water. On a global scale, the distribution of the water resources on Earth is given in Table 1.2, where it is clear that the vast majority of the Earth's water resources (97%) is contained in the oceans, with most of the freshwater being contained in groundwater and polar ice. Groundwater is a particularly important water resource, comprising more than 98% of the liquid freshwater available on Earth; less than 2% of liquid freshwater is contained in streams and lakes. The amount of water stored in

Table 1.1: Classes of Water Contaminants

Contaminant class	Example
Oxygen-demanding wastes	Plant and animal material
Infectious agents	Bacteria and viruses
Plant nutrients	Fertilizers, such as nitrates and phosphates
Organic chemicals	Pesticides, detergents, oil, grease
Inorganic chemicals	Acids from coal mine drainage, inorganic chemicals such as iron from steel plants
Sediment from land erosion	Clay silt on streambed, which may reduce or even destroy life forms living at the solid-liquid interface
Radioactive substances	Waste products from mining and processing of radioactive material, radioactive isotopes after use
Heat from industry	Cooling water used in steam generation of electricity

Table 1.2: Estimated World Water Quantities

Item	Volume ($\times 10^3$ km^3)	Percent total water (%)	Percent freshwater (%)
Oceans	1 338 000	96.5	
Groundwater			
Fresh	10 530	0.76	30.1
Saline	12 870	0.93	
Soil moisture	16.5	0.0012	0.05
Polar ice	24 023.5	1.7	68.6
Other ice and snow	340.6	0.025	1.0
Lakes			
Fresh	91	0.007	0.26
Saline	85.4	0.006	
Marshes	11.47	0.0008	0.03
Rivers	2.12	0.0002	0.006
Biological water	1.12	0.0001	0.003
Atmospheric water	12.9	0.001	0.04
Total water	1 385 984.61	100.00	
Freshwater	35 029.21	2.5	100.00

Source: USSR National Committee for the International Hydrological Decade (1978).

the atmosphere is relatively small, although the flux of water into and out of the atmosphere dominates the hydrologic cycle. The typical residence time for atmospheric water is on the order of a week, the typical residence time for soil moisture is on the order of weeks to months, and the typical residence time in the oceans is on the order of tens of thousands of years. The estimated fluxes of precipitation, evaporation, and runoff within the global hydrologic cycle are given in Table 1.3. These data indicate that the global average

Table 1.3: Fluxes in Global Hydrologic Cycle

Component	Oceanic flux (mm/yr)	Terrestrial flux (mm/yr)
Precipitation	1270	800
Evaporation	1400	484
Runoff to ocean (rivers plus groundwater)	—	316

Source: USSR National Committee for the International Hydrological Decade (1978).

precipitation over land is on the order of 800 mm/yr (31 in/yr), of which 484 mm/yr (19 in/yr) is returned to the atmosphere as evaporation, and 316 mm/yr (12 in/yr) is returned to the ocean via surface runoff. On a global scale, large variations from these average values are observed. In the United States, for example, the highest average annual rainfall is found at Mount Wai'ale'ale on the Hawaiian island of Kauai, with an annual rainfall of 1168 cm/yr (460 in/yr), while Greenland Ranch in Death Valley, California, has the lowest annual average rainfall of 4.5 cm/yr (1.8 in/yr). Globally, the highest (measured) annual average rainfall is at Mawsynram, India, with an average annual rainfall of 1187 cm/yr (467 in/yr). At Calama in the Atacama Desert in northern Chile, rainfall has never been recorded.

Relationship of water to climate. Two of the most widely used climatic measures are the mean annual rainfall and the mean annual potential evapotranspiration. A *climate spectrum* appropriate for subtropical and midlatitudinal regions is given in Table 1.4, and water-resources management differs substantially between climates. For example, forecasting and planning for drought conditions are particularly important in semiarid climates, whereas droughts are barely noticeable in hyperhumid climates. Climatic conditions also have a controlling influence on the water budget as shown in Figure 1.3. In humid climates, annual rainfall is high and surface runoff, groundwater recharge, and evapotranspiration (ET) are all significant processes. In comparison, in arid climates, annual rainfall is low, evapotranspiration is the dominant process, surface

Table 1.4: Climate Spectrum

Climate	Mean annual precipitation (mm)	Mean annual potential evapotranspiration (mm)	Length of rainy season (months)
Superarid	<100	>3000	<1
Hyperarid	100–200	2400–3600	1–2
Arid	200–400	2000–2400	2–3
Semiarid	400–800	1600–2000	3–4
Subhumid	800–1600	1200–1600	4–6
Humid	1600–3200	1200	6–9
Hyperhumid	3200–6400	1200	9–12
Superhumid	≥ 6400	1200	12

Source: Ponce et al. (2000).

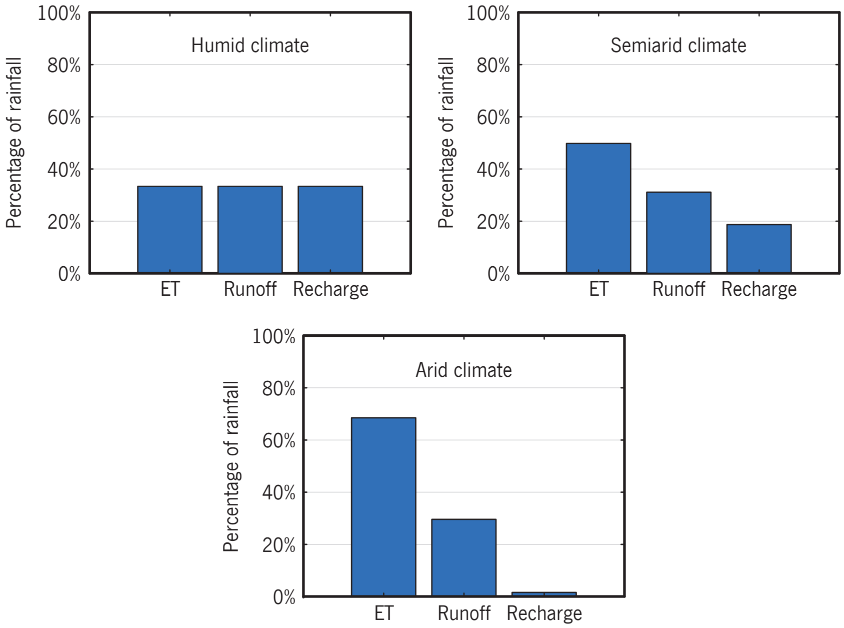

Figure 1.3: Typical water budgets in different climates

runoff is also important, and groundwater recharge is almost negligible. In semiarid climates, evapotranspiration remains the dominant process, although surface runoff and groundwater recharge are both important processes.

Management of water resources. On regional scales, water resources are usually managed within topographically defined areas called *watersheds* or *basins*. These areas are enclosed by topographic high points in the land surface, and within these bounded areas the path of surface runoff can usually be controlled with a reasonable degree of coordination. Human activities such as land-use changes, dam construction and reservoir operation, surface-water and groundwater withdrawal, and return flows within watersheds can have significant impacts on regional ecologies and should generally be taken into account in managing and designing water-resource systems.

1.3 Design of Water-Resource Systems

The uncertainty and natural variability of hydrologic processes require that most water-resource systems be designed with some degree of *risk* (of failure). Approaches to designing such systems can be classified as either *frequency-based design*, *risk-based design*, or *critical-event design*. In frequency-based design, the exceedance probability of the design event is selected a priori, and the water-resource system is designed to accommodate all lesser events up to and including the event with the selected exceedance probability. The water-resource system is then expected to fail with a probability equal to the exceedance probability of the design event. The frequency-based design approach is commonly used in designing minor structures in urban drainage systems. For example, urban storm-drainage systems are typically designed for precipitation events with return periods of 10 years or less, where the *return period* of an event is defined as the reciprocal of the (annual) exceedance probability of the event. In risk-based design, systems are designed such that the sum of the capital cost and the cost of failure is minimized. Capital costs tend to increase and the cost of failure tends to decrease with increasing system capacity. Because any threats to human life are generally assigned extremely high failure costs, structures such as large dams are usually designed for rare hydrologic events with long return periods and commensurate small failure risks. In some extreme cases, where the consequences of failure are truly catastrophic, water-resource systems are designed for the largest possible magnitude of a hydrologic event. This approach is called *critical-event design*, and the value of the design (hydrologic) variable in this case is referred to as the *estimated limiting value* (ELV).

1.4 Types of Water-Resource Systems

Water-resource systems can be broadly categorized as *water-control systems* or *water-use systems*, with corresponding design objectives as shown in Table 1.5; however, these systems are not mutually exclusive. The following sections present a brief overview of the design objectives in water-control and water-use systems.

1.4.1 Water-Control Systems

Water-control systems are primarily designed to control the spatial and temporal distribution of surface runoff resulting from rainfall events. Flood-control structures and storage impoundments reduce the peak flows in rivers, streams, and drainage channels, thereby reducing the occurrence of floods. A *flood* is defined as a high flow that exceeds the capacity of a stream, drainage channel, and/or flood-control structure; floods are usually associated with ground inundation. Extreme flooding is of major concern, since it usually leads to loss of life and large economic losses. The risk of extreme flooding at any given location tends to increase over time due to such key factors as population growth, urbanization, infrastructure decay, and climate change. The elevation at which water overflows the embankments of a stream or drainage channel is called the *flood stage*, and a *floodplain* is the normally dry land adjacent to rivers, streams, lakes, bays, or oceans that is inundated during flood events. Typically, flows with return periods in the range of 1.5–3 years represent bankfull conditions in natural streams, with larger flows causing inundation of the floodplain. The 100-year flood has been adopted by the U.S. Federal Emergency Management Agency (FEMA) as the base flood for delineating floodplains, and the area inundated by the 500-year flood is sometimes delineated to indicate additional areas at a lessened risk. Encroachment onto floodplains usually reduces the capacity of the watercourse, and increases the extent of the floodplain. Approximately 7–10% of the land in the United States is in a floodplain. The largest floodplain areas in the United States are in the South, and the most populated floodplains are along the north Atlantic coast, the Great Lakes region, and in California. In coastal areas, sea-level rise is expected to have a significant effect on flood frequencies. Sea-level rise will continue to contribute directly

Table 1.5: Design Objectives of Water-Resource Systems

Water-control systems	Water-use systems
Drainage	Domestic and industrial water supply
Flood control	Wastewater treatment
Salinity control	Irrigation
Sediment control	Hydropower generation
Pollution abatement	

to increases in storm surge, wave heights, and coastal erosion, all of which need to be addressed by either nonstructural or structural human interventions.

Urban water-control systems. In urban settings, water-control systems include storm-sewer systems for collecting and transporting surface runoff, and storage reservoirs that attenuate peak runoff rates and reduce pollutant loads in drainage channels. Urban stormwater-control systems are typically designed to prevent flooding from runoff events with return periods of 10 years or less. For runoff events that exceed the design event, surface (street) flooding usually results.

1.4.2 Water-Use Systems

Water-use systems are designed to support human habitation, and include: water-treatment systems, water-distribution systems, wastewater-collection systems, wastewater-treatment systems, and irrigation systems. Water for these systems are generally withdrawn from rivers, lakes, or groundwater; and great care must be taken to ensure that water withdrawals from these sources are sustainable. The design capacity of water-use systems is generally dictated by the population and characteristics of the service area, commercial and industrial requirements, crop requirements, and/or the economic design life of the system. Some key design aspects of these systems are given below.

Domestic water-supply systems. These systems typically include water-extraction facilities, such as wellfields, that must extract water from the source at rates that do not cause adverse effects on the source water and those that depend on it; water-treatment plants that must produce water of sufficient quality to meet drinking-water standards; and water-distribution systems that must meet peak demands while sustaining adequate water pressures.

Domestic wastewater-collection systems. Sanitary sewers and associated appurtenances must have sufficient capacity to transport wastes without overflowing into the streets or causing backups. These systems typically terminate at a wastewater-treatment plant or water-resource recovery facility that must provide a sufficient level of treatment for the intended use of the effluent, and effluent discharge systems that do not degrade the receiving waters.

Irrigation systems. In agricultural areas, the water requirements of crops are met by a combination of rainfall and irrigation. The design of irrigation systems requires the estimation of crop evapotranspiration rates and leaching requirements. Usually, irrigation water is obtained from groundwater, and care must be taken to ensure that the extraction rates are sustainable, and long-term declines in groundwater resources will not occur.

Hydroelectric power systems. In rivers and streams where there are large seasonal variations in flow rates, construction of dams and the generation of hydroelectric power might be economically feasible. In such cases, water reservoirs are sized to provide sufficient capacity to store excess water in years and seasons of surplus water, and provide water to support human habitation in years and seasons of water deficit. Water released from the storage reservoirs can be used to generate hydroelectric power, which is a clean, nonpolluting, and renewable source of electricity.

1.4.3 Supporting Federal Agencies in the United States

The design of water-resource systems usually involves interaction with government agencies. Collection of hydrologic and geologic data, granting of development permits, specification of design criteria, and use of government-developed computer codes for developing models of water-resource systems are some of the many areas in which water-resources engineers interact with government agencies. Some of the key federal water-resources agencies in the United States and their primary functions are given below.

National Climatic Data Center (NCDC). NCDC is the world's largest active source of weather data; it produces numerous climate publications, and responds to data requests from all over the world. Most of the data available from the NCDC are collected and analyzed by the National Weather Service (NWS), Military Services, Coast Guard, Federal Aviation Administration, and state and local government agencies.

U.S. Army Corps of Engineers (USACE). USACE is responsible for the planning, construction, operation, and maintenance of a variety of water-resource facilities whose objectives include navigation, flood control, water supply, recreation, hydroelectric power generation, water-quality control, and other purposes.

U.S. Bureau of Reclamation (USBR). USBR is responsible for planning, construction, operation, and maintenance of a variety of water-resource facilities whose objectives include irrigation, power generation, recreation, fish and wildlife preservation, and municipal water supply. Most of the USBR activities are confined to the 17 (arid) states west of the Mississippi River. Besides being the largest wholesale supplier of water in the United States, USBR is the sixth largest hydroelectric supplier in the United States.

U.S. Environmental Protection Agency (USEPA). USEPA is responsible for the implementation and enforcement of federal environmental laws. The agency's mission is to protect public health and to safeguard and improve the natural environment—air, water, and land—upon which human life depends.

U.S. Geological Survey (USGS). The Water Resources Division of the USGS has primary federal responsibility for collection and dissemination of measurements of stream discharge and stage, reservoir and lake stage and storage, groundwater levels, well and spring discharge, and the quality of surface and groundwater in the United States. USGS maintains a network of thousands of stream gages and groundwater monitoring wells. A particularly useful resource is the National Water Information System: Web Interface (https://waterdata.usgs.gov/nwis), where surface-water, groundwater, water-quality, and water-use data for the United States can be readily obtained.

U.S. National Weather Service (NWS). NWS, under the direction of the National Oceanic and Atmospheric Administration (NOAA), has a mandate to collect hydrologic data and provide weather, hydrologic, and climate forecasts. Data collected by NWS include rainfall, temperature, and evaporation measurements at over 10 000 locations in the United States. The NWS uses its River Forecast System at 13 River Forecast Centers to provide daily river-stage forecasts at approximately 4000 locations.

U.S. Natural Resources Conservation Service (NRCS). NRCS works with landowners on private lands to conserve natural resources. NRCS provides technical and financial assistance to farmers and ranchers for flood protection, recreation, and water-supply development in watersheds with areas less than

Table 1.6: Federal Agencies Relevant to Water-Resources Engineering in the United States

Organization	Web address
National Climatic Data Center (NCDC)	www.ncdc.noaa.gov
U.S. Army Corps of Engineers (USACE)	www.usace.army.mil
U.S. Bureau of Reclamation (USBR)	www.usbr.gov
U.S. Environmental Protection Agency (USEPA)	www.epa.gov
U.S. Geological Survey (USGS)	www.usgs.gov
U.S. National Weather Service (NWS)	www.nws.noaa.gov
U.S. Natural Resources Conservation Service (NRCS)	www.nrcs.usda.gov

1000 km^2 (400 mi^2). The NRCS publishes general soil maps for each state, and detailed soil maps for each county in the United States. The Snowpack Telemetry (SNOTEL) system operated by NRCS provides year-round temperature and precipitation data in remote, mountainous areas primarily in the western United States.

The aforementioned federal agencies provide a wealth of data and information on water resources, relevant government regulations, and useful computer software that can be found on the Internet. Agency Web sites currently in use (and likely to be around for the foreseeable future) are listed in Table 1.6.

Problem

1.1. Search the Internet to determine the mean annual rainfall and evapotranspiration of Boston, Massachusetts, and Santa Fe, New Mexico. Classify the climate in these cities.

Chapter 2

Fundamentals of Flow in Closed Conduits

2.1 Introduction

Closed-conduit flow occurs when a flowing fluid completely fills a conduit. The cross sections of closed conduits can be of any shape or size, and conduits can be made of any solid material. Engineering applications of the principles of flow in closed conduits include the design of water-supply systems, water-transmission lines, and building water-distribution systems. The basic equations governing the flow of fluids in closed conduits are the continuity, momentum, and energy equations, and the most useful forms of these equations for application to closed-conduit flow are derived in this chapter. The governing equations are presented in forms that are applicable to any fluid flowing in a closed conduit, but particular attention is given to the flow of water.

Pipe networks. Flows in pipe networks are a natural extension of flows in single pipelines, and methods of calculating flows and pressure distributions in pipeline systems are covered in this chapter. These methods are particularly applicable in the analysis and design of water-distribution systems, where the design engineer is frequently interested in assessing the effects of various modifications to the system.

Pumps. Transmission of water in closed conduits is typically driven by pumps, and the fundamentals of pump operation and performance are presented in this chapter. A sound understanding of pumps is important in selecting the appropriate pump to achieve the desired operational characteristics in water-transmission systems.

2.2 Single Pipelines

The governing equations for flows in pipelines are derived from the conservation laws of mass, momentum, and energy, and the forms of these equations that are most useful for application to closed-conduit flow are derived in the following sections.

2.2.1 Steady-State Continuity Equation

Consider the application of the law of conservation of mass to the control volume illustrated in Figure 2.1. Fluid enters and leaves the control volume normal to the control surface, with the inflow velocity denoted by

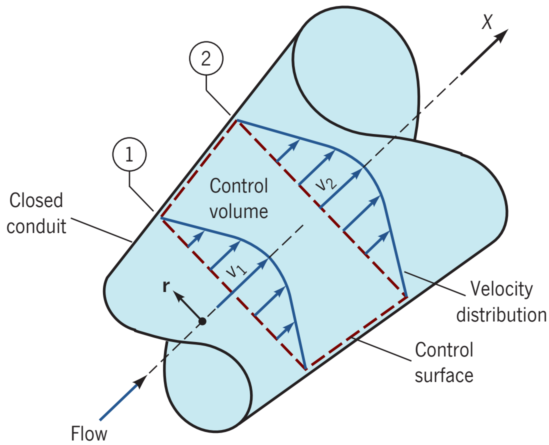

Figure 2.1: Flow through closed conduit

$v_1(\mathbf{r})$ and the outflow velocity by $v_2(\mathbf{r})$, where $\mathbf{r}$ is the radial position vector originating at the centerline of the conduit. Both the inflow and outflow velocities vary across the control surface. The analytic expression of the law of conservation of mass is generally referred to as the *continuity equation*, and the steady-state continuity equation for an incompressible fluid can be written as

$$\int_{A_1} \rho v_1 \, \mathrm{d}A = \int_{A_2} \rho v_2 \, \mathrm{d}A \tag{2.1}$$

where ρ is the (constant) density of the fluid flowing in the closed conduit. Defining V_1 and V_2 as the average velocities across A_1 and A_2, respectively, where

$$V_1 = \frac{1}{A_1}\int_{A_1} v_1 \, \mathrm{d}A, \qquad V_2 = \frac{1}{A_2}\int_{A_2} v_2 \, \mathrm{d}A \tag{2.2}$$

the steady-state continuity equation, Equation 2.1, can be expressed as

$$\boxed{V_1A_1 = V_2A_2 \; (= Q)} \tag{2.3}$$

where the terms on each side of Equation 2.3 are equal to the volumetric flow rate, Q. The steady-state continuity equation simply states that the volumetric flow rate across any surface normal to the flow is a constant.

Example 2.1
Water enters a pump through a 150-mm diameter intake pipe and leaves through a 200-mm diameter discharge pipe. If the average velocity in the intake pipe is 1 m/s, calculate the average velocity in the discharge pipe. What is the flow rate through the pump?

Solution.
From the given data: $D_1 = 0.15$ m, $D_2 = 0.20$ m, and $V_1 = 1$ m/s. The cross-sectional areas of the intake and discharge pipes are given by

$$A_1 = \frac{\pi}{4}D_1^2 = \frac{\pi}{4}(0.15)^2 = 0.0177\ \mathrm{m}^2, \qquad A_2 = \frac{\pi}{4}D_2^2 = \frac{\pi}{4}(0.20)^2 = 0.0314\ \mathrm{m}^2$$

According to the continuity equation,

$$V_1A_1 = V_2A_2 \quad \longrightarrow \quad V_2 = V_1\left(\frac{A_1}{A_2}\right) = (1)\left(\frac{0.0177}{0.0314}\right) = 0.56\,\text{m/s}$$

The flow rate, Q, through the pump is given by

$$Q = A_1V_1 = (0.0177)(1) = 0.0177\,\text{m}^3\text{/s} = 17.7\,\text{L/s}$$

The average velocity in the discharge pipe is **0.56 m/s**, and the flow rate through the pump is **17.7 L/s**.

Practicality. Volumetric flow rates of liquids in closed conduits are typically expressed in units of L/s (or gpm); since using the conventional units of volumetric flow rate (m^3/s or ft^3/s) would typically require numeric values that are much less than unity.

2.2.2 Steady-State Momentum Equation

The *momentum equation* is the analytic expression of Newton's second law of motion, which is sometimes called the law of conservation of momentum. Consider the application of the momentum equation to the control volume illustrated in Figure 2.1. Under steady-state conditions, the component of the momentum equation in the direction of flow (x-direction) can be written as

$$\sum F_x = \int_A \rho v_x(\mathbf{v}\cdot\mathbf{n})\,\mathrm{d}A \tag{2.4}$$

where $\sum F_x$ is the sum of the x-components of the forces acting on the fluid in the control volume, A is the area of the control surface, ρ is the density of the fluid, v_x is the component of the flow velocity in the x-direction, $\mathbf{v}$ is the velocity vector, $\mathbf{n}$ is the unit normal to the control surface and pointing outward from the control volume, and $\mathbf{v}\cdot\mathbf{n}$ is the component of the flow velocity normal to the control surface. Since the unit normal vector, $\mathbf{n}$, in Equation 2.4 is directed outward from the control volume, the momentum equation for an incompressible fluid (ρ = constant) can be expressed as

$$\sum F_x = \rho\int_{A_2} v_2^2\,\mathrm{d}A - \rho\int_{A_1} v_1^2\,\mathrm{d}A \tag{2.5}$$

where v_1 and v_2 are the inflow and outflow velocities, respectively, and the integral terms depend on the velocity distributions across the inflow and outflow control surfaces. The velocity distribution across each control surface is generally accounted for by the *momentum correction coefficient*, β, defined by the relation

$$\boxed{\beta = \frac{1}{AV^2}\int_A v^2\,\mathrm{d}A} \tag{2.6}$$

where A is the area of the control surface, and V is the average velocity over the control surface. The momentum correction coefficients for the inflow and outflow control surfaces, A_1 and A_2, are given by β_1 and β_2, where

$$\beta_1 = \frac{1}{A_1V_1^2}\int_{A_1} v_1^2\,\mathrm{d}A, \qquad \beta_2 = \frac{1}{A_2V_2^2}\int_{A_2} v_2^2\,\mathrm{d}A$$

Substituting these relations into Equation 2.5 leads to the following form of the momentum equation:

$$\sum F_x = \rho\beta_2 V_2^2 A_2 - \rho\beta_1 V_1^2 A_1 \tag{2.7}$$

Recalling that the continuity equation states that the volumetric flow rate, Q, is the same across both the inflow and outflow control surfaces, where

$$Q = V_1 A_1 = V_2 A_2 \tag{2.8}$$

then combining Equations 2.7 and 2.8 leads to the following useful form of the steady-state momentum equation:

$$\sum F_x = \rho\beta_2 Q V_2 - \rho\beta_1 Q V_1 \quad \rightarrow \quad \sum F_x = \rho Q(\beta_2 V_2 - \beta_1 V_1) \quad \rightarrow \quad \boxed{\sum F_x = \dot{m}(\beta_2 V_2 - \beta_1 V_1)}$$

where $\dot{m}$ is the mass flow rate in the closed conduit, which is equal to ρQ. In many cases of practical interest, the velocity distribution across the conduit cross section is approximately uniform, in which case the momentum correction coefficients, β_1 and β_2, are approximately equal to unity, and the steady-state momentum equation becomes

$$\boxed{\sum F_x = \dot{m}(V_2 - V_1)} \tag{2.9}$$

Consider the common case of flow in a straight conduit with a uniform circular cross section as illustrated in Figure 2.2, where the average velocity remains constant at each cross section,

$$V_1 = V_2 = V \tag{2.10}$$

then the steady-state momentum equation becomes

$$\sum F_x = 0 \tag{2.11}$$

This result reflects the condition that the fluid in the conduit is not accelerating, and therefore, the sum of the forces on the control volume is equal to zero.

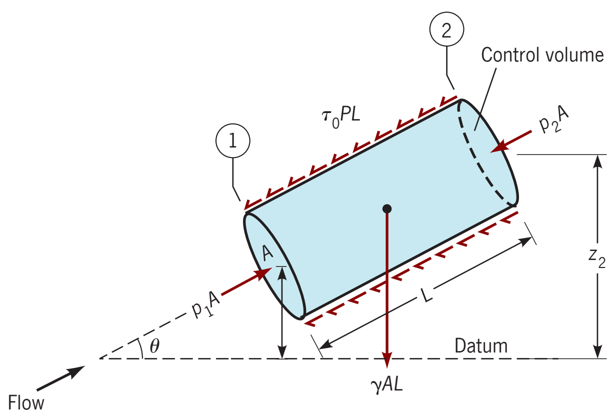

Figure 2.2: Forces on flow in closed conduit

Forces on the fluid in a control volume. The forces that act on the fluid in a control volume of uniform cross section are illustrated in Figure 2.2. At Section 1, the average pressure over the control surface is equal to p_1, and the elevation of the midpoint of the section relative to a defined datum is z_1. At Section 2, located a distance L downstream from Section 1, the average pressure is p_2, and the elevation of the midpoint of the section is z_2. The average shear stress exerted on the moving fluid by the stationary conduit surface is equal to τ_0, and the total shear force opposing the flow is $\tau_0 PL$, where P is the perimeter of the conduit. The fluid weight acts vertically downward and is equal to γAL, where γ is the specific weight of the fluid, and A is the cross-sectional area of the conduit. The forces acting on the fluid system that have components in the direction of flow are: the shear force, $\tau_0 PL$; the weight of the fluid in the control volume, γAL; and the pressure forces on the upstream and downstream faces, $p_1 A$ and $p_2 A$, respectively. Substituting the expressions for the forces into the momentum equation, Equation 2.11, yields

$$p_1 A - p_2 A - \tau_0 PL - \gamma AL \sin\theta = 0 \tag{2.12}$$

where θ is the angle that the conduit makes with the horizontal, and is given by the relation

$$\sin\theta = \frac{z_2 - z_1}{L} \tag{2.13}$$

Combining Equations 2.12 and 2.13 yields

$$\frac{p_1}{\gamma} - \frac{p_2}{\gamma} - z_2 + z_1 = \frac{\tau_0 PL}{\gamma A} \tag{2.14}$$

Defining the *total head*, or *mechanical energy per unit weight*, at sections 1 and 2 as h_1 and h_2, respectively, where

$$h_1 = \frac{p_1}{\gamma} + \frac{V^2}{2g} + z_1, \qquad h_2 = \frac{p_2}{\gamma} + \frac{V^2}{2g} + z_2$$

then the *head loss* between sections 1 and 2, Δh, is given by

$$\Delta h = h_1 - h_2 = \left(\frac{p_1}{\gamma} + z_1\right) - \left(\frac{p_2}{\gamma} + z_2\right) \tag{2.15}$$

Combining Equations 2.14 and 2.15 leads to the following expression for head loss in terms of the boundary shear stress:

$$\Delta h = \frac{\tau_0 PL}{\gamma A} \tag{2.16}$$

In this case, the head loss, Δh, is due entirely to friction between the flowing fluid and the pipe surface, and this head loss is commonly denoted by h_f, were the subscript "f" denotes the frictional cause of the head loss. The ratio of the cross-sectional area, A, to the perimeter, P, of the conduit is defined as the *hydraulic radius*, R, where

$$R = \frac{A}{P} \tag{2.17}$$

Combining Equations 2.16 and 2.17, the head loss due to friction can be written in terms of the hydraulic radius as

$$h_\mathrm{f} = \frac{\tau_0 L}{\gamma R} \tag{2.18}$$

For conduits with a circular cross section and diameter D, the hydraulic radius, R, is given by

$$R = \frac{A}{P} = \frac{\pi D^2/4}{\pi D} = \frac{D}{4} \tag{2.19}$$

in which case Equation 2.18 can be written as

$$h_\mathrm{f} = \frac{4\tau_0 L}{\gamma D} \qquad \text{(for circular conduits)} \tag{2.20}$$

Dimensional analysis. The form of the momentum equation given by Equation 2.18 is of limited utility in that the head loss, h_f, is expressed in terms of the boundary shear stress, τ_0, which is not an easily measurable quantity. The boundary shear stress, τ_0, can be expressed as a function of groups of measurable flow variables using dimensional analysis. For circular conduits of diameter D, the boundary shear stress, τ_0, can be assumed to be a function of the mean flow velocity, V; density of the fluid, ρ; dynamic viscosity of the fluid, μ; characteristic size of roughness projections, ϵ; characteristic spacing of the roughness projections, ϵ'; and a (dimensionless) form factor, m, that depends on the shape of the roughness elements on the surface of the conduit. This functional relation can be expressed as

$$\tau_0 = f_1(V, \rho, \mu, D, \epsilon, \epsilon', m) \tag{2.21}$$

According to the Buckingham pi theorem, this relation between eight variables in three fundamental dimensions (mass, length, and time) can also be expressed as a relation between five dimensionless groups. The following relation is proposed:

$$\frac{\tau_0}{\rho V^2} = f_2\left(\mathrm{Re}, \frac{\epsilon}{D}, \frac{\epsilon'}{D}, m\right) \tag{2.22}$$

where Re is the Reynolds number defined by

$$\mathrm{Re} = \frac{\rho V D}{\mu} \tag{2.23}$$

The relation given by Equation 2.22 is as far as dimensional analysis goes, and experiments are necessary to determine an empirical relation between the dimensionless groups. Nikuradse (1932; 1933) conducted a series of experiments on the turbulent flow of water in pipes, in which the inner surfaces were roughened with sand grains of uniform diameter, ϵ. In these experiments, the spacing, ϵ', and shape, m, of the roughness elements (sand grains) were constant, so Nikuradse's experimental data could be fitted to the following functional relation:

$$\frac{\tau_0}{\rho V^2} = f_3\left(\mathrm{Re}, \frac{\epsilon}{D}\right) \tag{2.24}$$

It is convenient for subsequent analysis to introduce a factor of $\frac{1}{8}$ into this relation, which can then be written as

$$\frac{\tau_0}{\frac{1}{8}\rho V^2} = f\left(\text{Re}, \frac{\epsilon}{D}\right) \quad \rightarrow \quad \tau_0 = f \cdot \tfrac{1}{8}\rho V^2 \tag{2.25}$$

where the dependence of the *friction factor*, f, on the Reynolds number, Re, and relative roughness, ϵ/D, is understood. Combining Equations 2.20 and 2.25 to eliminate τ_0 leads to the following form of the momentum equation for flows in circular pipes:

$$\boxed{h_\text{f} = \frac{fL}{D}\frac{V^2}{2g}} \tag{2.26}$$

This equation, called the *Darcy–Weisbach equation*,* expresses the frictional head loss, h_f, of the fluid over a length (L) of pipe in terms of measurable parameters, including the pipe diameter (D), the average flow velocity (V), and the friction factor (f) that is a function of the relative roughness (ϵ) and the Reynolds number (Re). Equation 2.26 is sometimes referred to simply as the Darcy equation; however, this is inappropriate, since it was Weisbach who first proposed the exact form of Equation 2.26 in 1845, with Darcy's contribution being the functional dependence of f on V and D in 1857 (Rouse and Ince, 1957; Brown, 2002). The values of f in laminar and turbulent flow were later quantified by Reynolds† in 1883 (Reynolds, 1883).

Nikuradse's experiments. Nikuradse (1932; 1933) performed seminal experiments to study the frictional head losses in pipes that were artificially roughened by sticking one layer of sand grains of uniform size onto the inner surfaces of smooth pipes. Based on Nikuradse's experimental results, Prandtl and von Kármán developed the following empirical equations for estimating the friction factor in turbulent pipe flows:

$$\boxed{\frac{1}{\sqrt{f}} = \begin{cases} -2\log\left(\dfrac{2.51}{\text{Re}\sqrt{f}}\right), & \text{Prandtl equation for smooth pipe } \left(\dfrac{k_\text{s}}{D} \approx 0\right) \\[2ex] -2\log\left(\dfrac{k_\text{s}/D}{3.7}\right), & \text{von Kármán equation for rough pipe } \left(\dfrac{k_\text{s}}{D} \gg 0\right) \end{cases}} \tag{2.27}$$

where k_s is the size of the sand grains on the surface of the pipe. Turbulent flow in pipes is generally present when $\text{Re} > 4000$, and transition to turbulent flow begins at about $\text{Re} = 2000$; laminar flow occurs when $\text{Re} < 2000$. A pipe behaves like a *smooth pipe* when the friction factor does not depend on the height of the roughness projections on the wall of the pipe, and therefore depends only on the Reynolds number. In *rough pipes*, the friction factor is determined solely by the relative roughness, k_s/D, and is independent of the Reynolds number. The smooth-pipe case generally occurs at lower Reynolds numbers, when the roughness projections are submerged within the laminar boundary layer adjacent to the pipe wall. At higher values of the Reynolds number, the thickness of the laminar boundary layer decreases, and eventually the roughness projections protrude sufficiently far outside the laminar boundary layer that the shear stress on the pipe wall is dominated by the hydrodynamic drag associated with the roughness projections into the

*Named in honor of the French engineer Henry Darcy (1803–1858) and the German engineer Julius Weisbach (1806–1871).
†Osbourne Reynolds (1842–1912) was a British engineer who made seminal contributions in the area of fluid dynamics.

main body of the flow. Under these circumstances, the flow in the pipe becomes *fully turbulent*, the friction factor is independent of the Reynolds number, and the pipe is considered to be (hydraulically) rough. The flow is actually turbulent under both smooth-pipe and rough-pipe conditions, but the flow is termed *fully turbulent* when the friction factor is independent of the Reynolds number. Between the smooth- and rough-pipe conditions, there is a transition region in which the friction factor depends on both the Reynolds number and the relative roughness.

The Colebrook equation. A limitation of Nikuradse's experiments on sand-roughened pipes was that the roughness heights were of uniform size, whereas in commercial pipes the roughness heights are generally nonuniform. Colebrook and White (1939) performed experiments on commercial pipes, and showed that head losses in commercial pipes could still be asymptotically characterized by the Prandtl and von Kármán equations (Equation 2.27); however, the transition region where f depends on both Re and k_s/D has a different behavior in commercial pipes than in Nikuradse's sand-roughened pipes. Colebrook (1939) identified the *equivalent sand roughness* of several commercial pipe materials that would give the same head losses as sand-roughened pipes under fully turbulent conditions, and developed the following relation that adequately describes the friction factor of commercial pipes under turbulent-flow conditions:

$$\frac{1}{\sqrt{f}} = -2\log\left(\frac{k_s/D}{3.7} + \frac{2.51}{\mathrm{Re}\sqrt{f}}\right) \tag{2.28}$$

This equation is commonly referred to as the *Colebrook equation* or the *Colebrook–White* equation. Values of friction factors, f, predicted by the Colebrook equation (Equation 2.28) are generally accurate to within 10–15% of experimental data, and the Colebrook equation asymptotes to the Prandtl and von Kármán equations given by Equation 2.27. The Colebrook equation is valid for estimating the friction factor for $4000 \leq \mathrm{Re} \leq 10^8$ and $0 \leq k_s/D \leq 0.1$. The accuracy of the Colebrook equation deteriorates significantly for small pipe diameters, and it is recommended that this equation not be used for pipes with diameters less than 2.5 mm (0.1 in) (Yoo and Singh, 2005). The Colebrook equation is valid only for turbulent flow (rough, smooth, and transition between rough and smooth). In cases where the flow is in the laminar-turbulent transition region, alternative approximations should be used (e.g., Cheng, 2008); however, such conditions are rare in hydraulic engineering.

Surface roughness. The equivalent sand roughness, k_s, of several commercial pipe materials is given in Table 2.1. These values of k_s apply to clean new pipe only; pipe that has been in service for a long time usually experiences corrosion or scale buildup that results in values of k_s that are orders of magnitude greater than the values given in Table 2.1. An example of the large roughness heights that can occur from scale buildup in public water-supply pipe is shown in Figure 2.3. It is apparent from Figure 2.3 that the increased roughness is of sufficient magnitude to also reduce the effective diameter of the pipe. In general, the rate of increase of the equivalent sand roughness, k_s, of a water-supply pipe with time depends primarily on the quality of the water being transported. The roughness coefficients for older water mains are usually determined through field testing.

Table 2.1: Typical Equivalent Sand Roughness for Various Materials

Material	Equivalent sand roughness, k_s (mm)
Asbestos cement:	
Coated	0.038
Uncoated	0.076
Brass	0.0015–0.003
Brick	0.6–6.0
Concrete:	
General	0.3–3.0
Steel forms	0.18
Wooden forms	0.6
Centrifugally spun	0.13–0.36
Clay	0.03–0.15
Copper	0.0015–0.003
Corrugated metal	45
Glass	0.0015–0.003
Iron:	
Cast iron	
General	0.2–5.5
Lined with asphalt	0.1–2.1
Uncoated	0.226
Coated	0.102
Ductile iron	0.26
Lined with bitumen	0.12
Lined with spun concrete	0.030–0.038
Galvanized iron	0.102–4.6
Wrought iron	0.046–2.4
Lead	0.0015
Plastic	0.0015–0.06
PVC	0.0015
Rubber, smoothed	0.01
Steel:	
Coal-tar enamel	0.0048
Commercial	0.045
New unlined	0.028–0.076
Riveted	0.9–9.0
Stainless	0.002
Wood stave	0.18–0.5

Sources: Butler and Davies (2011); Çengel and Cimbala (2014); Haestad et al., (2004); Haestad Methods, Inc. (2002); Moody (1944); Sanks (1998).

Figure 2.3: Corroded pipe
Source: Courtesy of Robert J. Ori, Public Resources Management Group, Inc.

Moody diagram. The expression for the friction factor given by the Colebrook equation (Equation 2.28) was plotted by Moody (1944) in what is commonly referred to as the *Moody diagram*[*] or *Moody chart*, reproduced in Figure 2.4. The Moody diagram indicates that for Re $\leq$ 2000, the flow is laminar, and the friction factor is given by

$$f = \frac{64}{\mathrm{Re}} \tag{2.29}$$

which is commonly known as the *Hagen–Poiseuille equation*, which can be derived theoretically based on the assumption of laminar flow of a Newtonian fluid (Chin, 2016). For 2000 $<$ Re $\leq$ 4000 there is no fixed relation between the friction factor and the Reynolds number or relative roughness, and flow conditions are generally uncertain. Beyond a Reynolds number of 4000, the flow is turbulent, and the friction factor is controlled by the thickness of the laminar boundary layer relative to the height of the roughness projections on the surface of the pipe. The dashed line in Figure 2.4 indicates the boundary between the fully turbulent-flow regime, where f is independent of Re, and the transition regime, where f depends on both Re and the relative roughness, k_s/D. The equation of this dashed line is given by (Mott, 2006)

$$\frac{1}{\sqrt{f}} = \frac{\mathrm{Re}}{200(D/k_s)} \tag{2.30}$$

The line in the Moody diagram corresponding to a relative roughness of zero describes the friction factor for pipes that are hydraulically smooth.

[*] Named after Lewis F. Moody (1880–1953). This type of diagram was originally suggested by Blasius in 1913 and Stanton in 1914 (Stanton and Pannell, 1914). The Moody diagram is sometimes called the *Stanton diagram*.

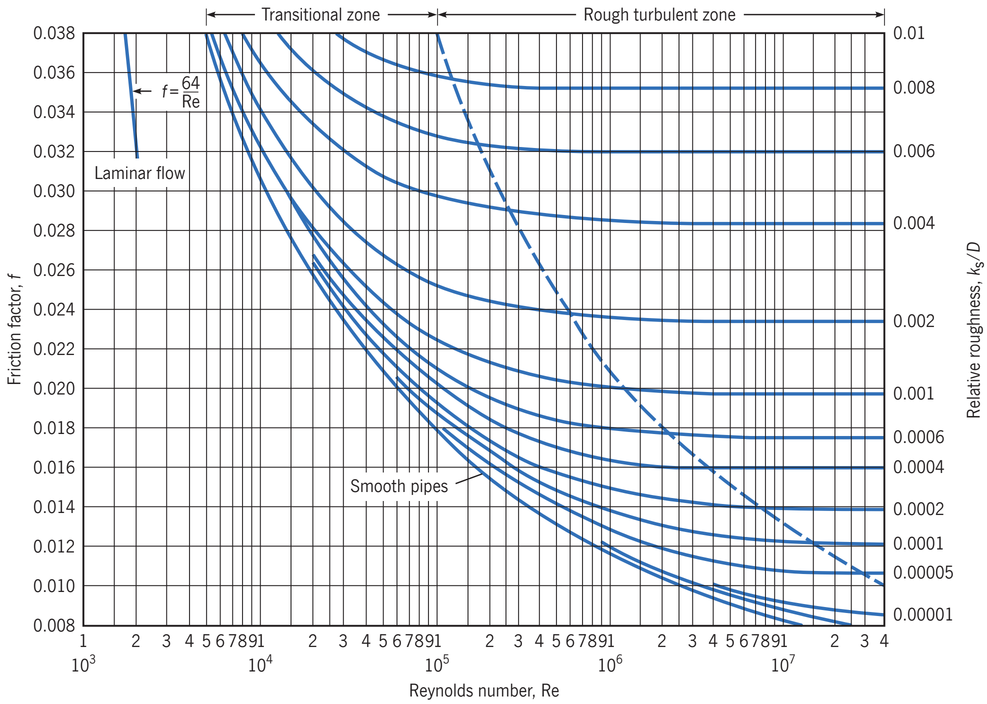

Figure 2.4: Moody diagram

Source: Moody (1944).

Swamee–Jain equation. Although the Colebrook equation (Equation 2.28) can be used to calculate the friction factor, this equation has the drawback that it is an implicit equation for the friction factor, and therefore must be solved numerically. This minor inconvenience was circumvented by Swamee and Jain (1976), who suggested the following explicit equation for the friction factor:

$$\frac{1}{\sqrt{f}} = -2\log\left(\frac{k_s/D}{3.7} + \frac{5.74}{\mathrm{Re}^{0.9}}\right), \quad \text{for } 10^{-6} \leq \frac{k_s}{D} \leq 0.01,\ 5000 \leq \mathrm{Re} \leq 10^8 \tag{2.31}$$

where, according to Swamee and Jain (1976), Equation 2.31 deviates by less than 1% from the Colebrook equation within the entire turbulent-flow regime, provided that the restrictions on k_s/D and Re are honored. The *Swamee–Jain equation* (Equation 2.31) can be more conveniently written as

$$f = \frac{0.25}{\left[\log\left(\frac{k_s}{3.7D} + \frac{5.74}{\mathrm{Re}^{0.9}}\right)\right]^2} \tag{2.32}$$

In addition to the Swamee–Jain equation, several other explicit equations have been proposed that approximate, to within about 1%, the friction factor given by the Colebrook equation (e.g., Haaland, 1983; Sonnad and Goudar, 2006). Uncertainties in the relative roughness and in the data used to produce the Colebrook equation make the use of several-significant-digit accuracy in estimating the friction factor unjustified. As a rule of thumb, an accuracy of 10% or no more that three significant digits in calculating the friction factor from either the Colebrook equation or close approximations is to be expected.

Example 2.2

Water from a treatment plant is pumped into a distribution system at a rate of 500 L/s, a pressure of 480 kPa, and a temperature of 20°C. The pipe has zero slope, a diameter of 750 mm, and is made of ductile iron. (a) Estimate the pressure 200 m downstream of the treatment plant. (b) Compare the friction factor estimated using the Colebrook equation to the friction factor estimated using the Swamee–Jain equation. (c) After 20 years in operation, scale buildup in the pipe is expected to cause the equivalent sand roughness to increase by a factor of 10; determine the effect on the water pressure 200 m downstream of the treatment plant.

Solution.

From the given data: $Q = 500\,\text{L/s} = 0.5\,\text{m}^3\text{/s}$, $p_1 = 480\,\text{kPa}$, $D = 0.75\,\text{m}$, and $L = 200\,\text{m}$. For ductile iron pipe, take $k_s = 0.26\,\text{mm}$. For water at 20°C, $\gamma = 9.79\,\text{kN/m}^3$ and $\upsilon = 1.00\times10^{-6}\,\text{m}^2\text{/s}$. The following preliminary calculations are useful:

$$A = \frac{\pi}{4}D^2 = \frac{\pi}{4}(0.75)^2 = 0.442\,\text{m}^2, \qquad V = \frac{Q}{A} = \frac{0.5}{0.442} = 1.13\,\text{m/s}$$

$$\text{Re} = \frac{VD}{\upsilon} = \frac{(1.13)(0.75)}{1.00\times10^{-6}} = 8.48\times10^5, \qquad \frac{k_s}{D} = \frac{0.26}{750} = 3.47\times10^{-4}$$

(a) Substituting into the Colebrook equation gives

$$\frac{1}{\sqrt{f}} = -2\log\left[\frac{k_s/D}{3.7} + \frac{2.51}{\text{Re}\sqrt{f}}\right] = -2\log\left[\frac{3.47\times10^{-4}}{3.7} + \frac{2.51}{8.48\times10^5\sqrt{f}}\right] \quad\rightarrow\quad f = 0.0161$$

The head loss, h_f, between the upstream and downstream sections can be calculated using the Darcy–Weisbach equation as

$$h_f = \frac{fL}{D}\frac{V^2}{2g} = \frac{(0.0161)(200)}{0.75}\frac{(1.13)^2}{(2)(9.81)} = 0.279\,\text{m}$$

Using the definition of head loss, h_f,

$$h_f = \left(\frac{p_1}{\gamma} + z_1\right) - \left(\frac{p_2}{\gamma} + z_2\right)$$

Since the pipe has zero slope, $z_1 = z_2$, and h_f can be written in terms of the pressures at the upstream and downstream sections as

$$h_f = \frac{p_1}{\gamma} - \frac{p_2}{\gamma} \quad\rightarrow\quad 0.279 = \frac{480}{9.79} - \frac{p_2}{9.79} \quad\rightarrow\quad p_2 = 477\,\text{kPa}$$

Therefore, the pressure 200 m downstream of the treatment plant is **477 kPa**.

(b) The Swamee–Jain approximation for f is given by

$$\frac{1}{\sqrt{f}} = -2\log\left[\frac{k_s/D}{3.7} + \frac{5.74}{\text{Re}^{0.9}}\right] \quad\rightarrow\quad \frac{1}{\sqrt{f}} = -2\log\left[\frac{3.47\times10^{-4}}{3.7} + \frac{5.74}{(8.48\times10^5)^{0.9}}\right] \quad\rightarrow\quad f = 0.0163$$

Comparing the f-values obtained using the Colebrook and Swamee–Jain equations (0.0161 versus 0.0163), it is apparent that the Swamee–Jain equation gives an f-value that is approximately **1% greater** than that given by the Colebrook equation.

(c) After 20 years, the equivalent sand roughness, k_s, of the pipe is 2.6 mm, and the Colebrook equation gives

$$\frac{1}{\sqrt{f}} = -2\log\left[\frac{2.6/750}{3.7} + \frac{2.51}{8.48\times10^5\sqrt{f}}\right] \quad\rightarrow\quad f = 0.0274$$

The head loss, h_f, between the upstream and downstream sections is given by the Darcy–Weisbach equation as

$$h_f = \frac{fL}{D}\frac{V^2}{2g} = \frac{(0.0274)(200)}{0.75}\frac{(1.13)^2}{(2)(9.81)} = 0.476\,\text{m}$$

Hence the pressure, p_2, 200 m downstream of the treatment plant is given by

$$h_f = \frac{p_1}{\gamma} - \frac{p_2}{\gamma} \quad\rightarrow\quad 0.476 = \frac{480}{9.79} - \frac{p_2}{9.79} \quad\rightarrow\quad p_2 = 475\,\text{kPa}$$

Therefore, pipe aging over 20 years will cause the pressure 200 m downstream of the treatment plant to decrease from 477 kPa to **475 kPa**, which is a decline of approximately 0.4%.

The previous example illustrates the case where the flow rate through a pipe is known, and the objective is to calculate the pressure drop over a given length of the pipe. The steps followed in the solution process are summarized as follows:

Step 1: Calculate the Reynolds number, Re, and the relative roughness, k_s/D, from the given data.

Step 2: Use the Colebrook equation (Equation 2.28) or Swamee–Jain equation (Equation 2.31) to calculate the friction factor, f.

Step 3: Use the calculated value of f to calculate the head loss using the Darcy–Weisbach equation (Equation 2.26), and calculate the corresponding pressure drop using Equation 2.15.

Flow rate for a given head loss. In many cases, the flow rate through a pipe is not directly controlled, but attains a flow rate that equilibrates to an externally imposed pressure drop. For example, the flow rate through a faucet in home plumbing equilibrates to the pressure drop in the service line between the pressurized water main at one end and the atmosphere at the other end. A useful approach to this problem that uses the Colebrook equation has been suggested by Fay (1994), where the first step is to calculate $\text{Re}\sqrt{f}$ using the rearranged Darcy–Weisbach equation

$$\text{Re}\sqrt{f} = \left(\frac{2gh_\text{f}D^3}{\nu^2 L}\right)^{\frac{1}{2}} \tag{2.33}$$

Using this value of $\text{Re}\sqrt{f}$, solve for Re using the rearranged Colebrook equation

$$\text{Re} = -2.0(\text{Re}\sqrt{f})\log\left(\frac{k_\text{s}/D}{3.7} + \frac{2.51}{\text{Re}\sqrt{f}}\right) \tag{2.34}$$

Using this value of Re, the flow rate, Q, can then be calculated by

$$Q = \frac{1}{4}\pi D^2 V = \frac{1}{4}\pi D\nu\text{Re} \tag{2.35}$$

This approach must necessarily be validated by verifying that $\text{Re} > 4000$, which is required for application of the Colebrook equation. Equations 2.33–2.35 yield the following combined form of the Darcy–Weisbach and Colebrook equations:

$$Q = -2.221D^2\sqrt{\frac{gDh_\text{f}}{L}}\log\left(\frac{k_\text{s}/D}{3.7} + \frac{1.775\nu}{D\sqrt{gDh_\text{f}/L}}\right) \tag{2.36}$$

where the coefficient of -2.221 is equal to $\pi\sqrt{2}/2$, and 1.775 is equal to $2.51/\sqrt{2}$. Equation 2.36 is dimensionally homogeneous, and is particularly useful since the flow rate, Q, can be explicitly calculated for given values of D, h_f/L, and k_s/D. Equation 2.36 can be appropriately called the *Darcy–Weisbach–Colebrook equation*.

Example 2.3
A 50-mm diameter galvanized iron service pipe is connected to a water main in which the pressure is 450 kPa. If the length of the service pipe to a faucet is 40 m, and the faucet is 1.2 m above the main, estimate the flow rate when the faucet is fully open.

Solution.
From the given data: $D = 50\,\text{mm} = 0.05\,\text{m}$, $p_1 = 450\,\text{kPa}$, $p_2 = 0\,\text{kPa}$, $L = 40\,\text{m}$, and $\Delta z = 1.2\,\text{m}$. For galvanized iron, $k_s = 0.15\,\text{mm}$ (from Table 2.1). Assume water at 20°C, so $\gamma = 9.79\,\text{kN/m}^3$ and $\upsilon = 1.00\times10^{-6}\,\text{m}^2/\text{s}$. The head loss, h_f, in the pipe is estimated by

$$h_f = \frac{p_1}{\gamma} - \left(\frac{p_2}{\gamma} + \Delta z\right) = \frac{450}{9.79} - \left(\frac{0}{9.79} + 1.2\right) = 44.8\,\text{m}$$

The combined Darcy–Weisbach–Colebrook equation (Equation 2.36) gives

$$Q = -2.221D^2\sqrt{\frac{gDh_f}{L}}\log\left[\frac{k_s/D}{3.7} + \frac{1.775\upsilon}{D\sqrt{gDh_f/L}}\right]$$

$$= -2.221(0.05)^2\sqrt{\frac{(9.81)(0.05)(44.8)}{40}}\log\left[\frac{0.15/50}{3.7} + \frac{1.775(1.00\times10^{-6})}{(0.05)\sqrt{(9.81)(0.05)(44.8)/40}}\right] = 0.0126\,\text{m}^3/\text{s} = 12.6\,\text{L/s}$$

The faucet can therefore be expected to deliver **12.6 L/s** when fully open.

Diameter for a given flow rate and head loss. In many cases, the design engineer must select a size of pipe to provide a specified flow rate. For example, the minimum required flow rate for an available head loss might be specified for a water delivery pipe, and the design engineer desires to calculate the minimum diameter pipe that will satisfy this design constraint. This is the usual design problem in gravity-driven pipelines. Solution of this design problem necessarily requires a numerical procedure, and can be easily accomplished by using a programmable calculator, a spreadsheet with solver capability, or a numerical computing environment such as MATLAB®.

Example 2.4
A galvanized iron service pipe from a water main is required to deliver 200 L/s during a fire. If the length of the service pipe is 35 m, and the head loss in the pipe is not to exceed 50 m, calculate the minimum pipe diameter that can be used.

Solution.
From the given data: $Q = 200\,\text{L/s} = 0.2\,\text{m}^3/\text{s}$, $L = 35\,\text{m}$, and $h_f = 50\,\text{m}$. Assume that $\upsilon = 1.00\times10^{-6}\,\text{m}^2/\text{s}$ (at 20°C), and take $k_s = 0.15\,\text{mm} = 1.5\times10^{-4}\,\text{m}$ (from Table 2.1). Substituting these data into Equation 2.36 gives

$$Q = -2.221D^2\sqrt{\frac{gDh_f}{L}}\log\left[\frac{k_s/D}{3.7} + \frac{1.775\upsilon}{D\sqrt{gDh_f/L}}\right]$$

$$0.2 = -2.221D^2\sqrt{\frac{(9.81)D(50)}{35}}\log\left[\frac{1.5\times10^{-4}/D}{3.7} + \frac{1.775(1.00\times10^{-6})}{D\sqrt{(9.81)D(50)/(35)}}\right]$$

This is an implicit equation in D that can be solved numerically to yield $D =$ **136 mm**.

Most numerical procedures that could be used for obtaining D in the previous example converge fairly quickly, and do not pose any computational difficulties. In lieu of determining an exact numerical solution, Swamee and Jain (1976) have suggested the following explicit equation for calculating the pipe diameter, D:

$$D = 0.66 \left[k_s^{1.25} \left(\frac{LQ^2}{gh_f} \right)^{4.75} + \upsilon Q^{9.4} \left(\frac{L}{gh_f} \right)^{5.2} \right]^{0.04} \tag{2.37}$$

Equation 2.37 is dimensionally homogeneous, is valid for $4000 \leq \text{Re} \leq 3\times10^8$ and $10^{-6} \leq k_s/D \leq 2\times10^{-2}$, and will yield a D within 5% of the value obtained by an exact solution to the Darcy–Weisbach and Colebrook equations. Use of Equation 2.37 is illustrated by repeating the previous example.

Example 2.5

A galvanized iron service pipe from a water main is required to deliver 200 L/s during a fire. If the length of the service pipe is 35 m, and the head loss in the pipe is not to exceed 50 m, use the Swamee–Jain approximation to calculate the minimum pipe diameter that can be used.

Solution.

Since $k_s = 0.15$ mm $= 1.5\times10^{-4}$ m, $L = 35$ m, $Q = 0.2$ m^3/s, $h_f = 50$ m, $\upsilon = 1.00\times10^{-6}$ m^2/s, the Swamee–Jain approximation (Equation 2.37) gives

$$\begin{aligned} D &= 0.66 \left\{ k_s^{1.25} \left[\frac{LQ^2}{gh_f} \right]^{4.75} + \upsilon Q^{9.4} \left[\frac{L}{gh_f} \right]^{5.2} \right\}^{0.04} \\ &= 0.66 \left\{ (1.5\times10^{-4})^{1.25} \left[\frac{(35)(0.2)^2}{(9.81)(50)} \right]^{4.75} + (1.00\times10^{-6})(0.2)^{9.4} \left[\frac{35}{(9.81)(50)} \right]^{5.2} \right\}^{0.04} = 0.140 \text{ m} = 144 \text{ mm} \end{aligned}$$

The calculated pipe diameter (**140 mm**) is about 3% higher than that calculated by simultaneous solution of the Darcy–Weisbach and Colebrook equations (i.e., 136 mm).

Note: The value of D obtained using the Darcy–Weisbach and Colebrook equations is generally more accurate than the value of D obtained using the Swamee–Jain approximation, and is therefore preferable to use the Darcy-Weisbach and Colebrook equations in design calculations.

2.2.3 Steady-State Energy Equation

Generalized flow conditions between two sections of a closed conduit are illustrated in Figure 2.5. Between the upstream and downstream sections (sections 1 and 2) there can be an exchange of heat between the fluid and the conduit, and there can also be a machine, such as a pump or turbine, that inputs or extracts energy from the flowing fluid. The steady-state energy equation for the control volume shown in Figure 2.5 is the analytic expression of the *first law of thermodynamics*, also called the *law of conservation of energy*, which can be expressed as

$$\dot{Q} - \dot{W} = \int_A \rho e \, (\mathbf{v}\cdot\mathbf{n}) \, dA \tag{2.38}$$

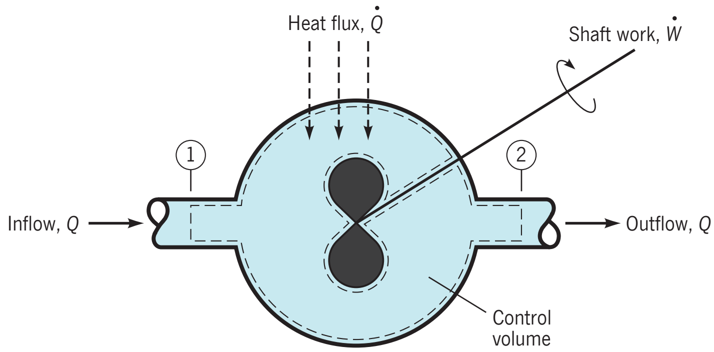

Figure 2.5: Energy balance in closed conduit

where $\dot{Q}$ is the rate at which heat is added to the fluid in the control volume, $\dot{W}$ is the rate at which work is done by the fluid in the control volume, A is the surface area of the control volume, ρ is the density of the fluid in the control volume, and e is the internal energy per unit mass of fluid in the control volume, which can be expressed as

$$e = gz + \frac{v^2}{2} + u \tag{2.39}$$

where z is the elevation of the fluid mass having a velocity v, g is the gravity constant, and u is the internal energy per unit mass. By convention, the heat added to a system and the work done by a system are positive quantities. The normal stresses on the inflow and outflow boundaries of the control volume are equal to the pressure, p, with shear stresses tangential to the boundaries of the control volume. As the fluid moves across the control surface with velocity $\mathbf{v}$, the power, $\dot{W}_\mathrm{p}$, expended by the fluid against the external pressure forces is given by

$$\dot{W}_\mathrm{p} = \int_A p(\mathbf{v}\cdot\mathbf{n})\,\mathrm{d}A \tag{2.40}$$

The rate of doing work (i.e., power) expended by a fluid in the control volume is typically separated into the power expended against external pressure forces, $\dot{W}_\mathrm{p}$, plus the power expended against rotating surfaces, $\dot{W}_\mathrm{s}$, commonly referred to as the *shaft power*. In a pump, the rotating element is called an *impeller*, and in a hydraulic turbine the rotating element is called a *runner*. The total power expended by a fluid system, $\dot{W}$, can therefore be expressed as

$$\dot{W} = \dot{W}_\mathrm{p} + \dot{W}_\mathrm{s} \quad \longrightarrow \quad \dot{W} = \int_A p(\mathbf{v}\cdot\mathbf{n})\,\mathrm{d}A + \dot{W}_\mathrm{s} \tag{2.41}$$

Combining Equation 2.41 with the steady-state energy equation (Equation 2.38), and substituting the definition of the internal energy, e, given by Equation 2.39 yields

$$\dot{Q} - \dot{W}_\mathrm{s} = \int_A \rho\left(\frac{p}{\rho} + gz + u + \frac{v^2}{2}\right)(\mathbf{v}\cdot\mathbf{n})\,\mathrm{d}A \tag{2.42}$$

The term $p/\rho + gz + u = g(p/\gamma + z) + u$ can be assumed to be constant across the inflow and outflow control surfaces, since the hydrostatic pressure distribution across the inflow/outflow boundaries guarantees that

$p/\gamma + z$ is constant across the boundaries, and the internal energy, u, depends only on the temperature of the fluid, which can be assumed constant across each boundary. Since $\mathbf{v}\cdot\mathbf{n}$ is equal to zero over the impervious boundaries in contact with the fluid system, Equation 2.42 simplifies to

$$\dot{Q} - \dot{W}_\mathrm{s} = \left[\frac{p}{\rho} + gz + u\right]_1 \int_{A_1} \rho(\mathbf{v}\cdot\mathbf{n})\,\mathrm{d}A + \int_{A_1} \rho\,\frac{v^2}{2}\,(\mathbf{v}\cdot\mathbf{n})\,\mathrm{d}A + \left[\frac{p}{\rho} + gz + u\right]_2 \int_{A_2} \rho(\mathbf{v}\cdot\mathbf{n})\,\mathrm{d}A + \int_{A_2} \rho\,\frac{v^2}{2}\,(\mathbf{v}\cdot\mathbf{n})\,\mathrm{d}A \quad (2.43)$$

where the subscripts 1 and 2 indicate the values of various quantities at the inflow and outflow boundaries, respectively. Equation 2.43 can be further simplified by noting that the assumption of steady state requires that the rate of mass inflow, $\dot{m}$, to the control volume is equal to the rate of mass outflow, where

$$\dot{m} = \int_{A_2} \rho\,(\mathbf{v}\cdot\mathbf{n})\,\mathrm{d}A = -\int_{A_1} \rho\,(\mathbf{v}\cdot\mathbf{n})\,\mathrm{d}A \quad (2.44)$$

and the negative sign comes from the fact that the unit normal points out of the control volume. The *kinetic energy correction coefficient*, α, for any cross section can be defined by

$$\alpha = \frac{1}{\frac{1}{2}\rho V^3 A} \int_A \tfrac{1}{2}\rho\,v^3\,\mathrm{d}A \quad \longrightarrow \quad \alpha = \frac{1}{A}\int_A \left(\frac{v}{V}\right)^3 \mathrm{d}A \quad (2.45)$$

where A is the flow area, and V is the mean velocity over the flow area; the density is assumed to be constant and cancels out. The kinetic energy correction coefficients at the inflow and outflow sections, α_1 and α_2, are determined by the velocity profiles across the inflow and outflow boundaries, respectively. If the velocity is constant across a flow boundary, then it is apparent from Equation 2.45 that the kinetic energy correction coefficient for that boundary is equal to unity; for any other velocity distribution, the kinetic energy factor is greater than unity. Combining Equations 2.43–2.45 leads to

$$\dot{Q} - \dot{W}_\mathrm{s} = -\left[\frac{p}{\rho} + gz + u\right]_1 \dot{m} - \alpha_1 \rho\,\frac{V_1^3}{2} A_1 + \left[\frac{p}{\rho} + gz + u\right]_2 \dot{m} + \alpha_2 \rho\,\frac{V_2^3}{2} A_2 \quad (2.46)$$

where the negative signs come from the convention that the unit normal points out of the control volume, making $\mathbf{v}\cdot\mathbf{n}$ negative for the inflow boundary in Equation 2.43. Invoking the steady-state continuity equation,

$$\rho V_1 A_1 = \rho V_2 A_2 = \dot{m} \quad (2.47)$$

Combining Equations 2.46 and 2.47 and rearranging gives

$$\frac{\dot{Q}}{\dot{m}g} - \frac{\dot{W}_\mathrm{s}}{\dot{m}g} = \left(\frac{p_2}{\gamma} + \frac{u_2}{g} + z_2 + \alpha_2\frac{V_2^2}{2g}\right) - \left(\frac{p_1}{\gamma} + \frac{u_1}{g} + z_1 + \alpha_1\frac{V_1^2}{2g}\right) \quad (2.48)$$

which can be further rearranged into the useful form:

$$\left(\frac{p_1}{\gamma} + \alpha_1\frac{V_1^2}{2g} + z_1\right) = \left(\frac{p_2}{\gamma} + \alpha_2\frac{V_2^2}{2g} + z_2\right) + \underbrace{\left[\frac{1}{g}(u_2 - u_1) - \frac{\dot{Q}}{\dot{m}g}\right]}_{=\text{ head loss, } h_\ell} + \underbrace{\left[\frac{\dot{W}_\mathrm{s}}{\dot{m}g}\right]}_{=\text{ shaft work, } h_\mathrm{s}} \quad (2.49)$$

Two key terms can be identified in Equation 2.49: the head loss, h_ℓ, and the (shaft) work done by the fluid per unit weight, h_s, where h_ℓ and h_s are defined by the relations

$$h_\ell = \frac{1}{g}(u_2 - u_1) - \frac{\dot{Q}}{\dot{m}g}, \qquad h_s = \frac{\dot{W}_s}{\dot{m}g} \tag{2.50}$$

Combining Equations 2.49 and 2.50 leads to the most common form of the steady-state *energy equation* for flow in closed conduits:

$$\left(\frac{p_1}{\gamma} + \alpha_1\frac{V_1^2}{2g} + z_1\right) = \left(\frac{p_2}{\gamma} + \alpha_2\frac{V_2^2}{2g} + z_2\right) + h_\ell + h_s \tag{2.51}$$

where a positive head loss, h_ℓ, indicates an increase in internal energy (manifested by an increase in temperature) and/or a loss of heat, and a positive shaft head, h_s, is associated with work being done by the fluid, such as in moving a turbine runner. The energy equation, Equation 2.51, states that the mechanical energy in a closed conduit is continuously being converted into thermal energy via head loss. Some practitioners incorrectly refer to Equation 2.51 as the *Bernoulli equation*, which bears some resemblance to Equation 2.51, but is different in several important respects. Fundamental differences between the energy equation and the Bernoulli equation are: (1) the Bernoulli equation is derived from the momentum equation, which is independent of the energy equation, (2) the Bernoulli equation does not account for fluid friction, and (3) the Bernoulli equation is applicable only for flow along a streamline.

2.2.3.1 Energy and hydraulic grade lines

The *total head*, h, of a fluid at any cross section of a pipe is defined by

$$h = \frac{p}{\gamma} + \alpha\frac{V^2}{2g} + z \tag{2.52}$$

where p is the pressure in the fluid at the centroid of the cross section, γ is the specific weight of the fluid, α is the kinetic energy correction coefficient, V is the average velocity across the pipe cross section, and z is the elevation of the centroid of the pipe cross section. The total head, h, measures the average mechanical energy per unit weight of the fluid at a pipe cross section. The energy equation, Equation 2.51, states that changes in the total head along the pipe are described by

$$h(x + \Delta x) = h(x) - (h_\ell + h_s) \tag{2.53}$$

where x is the coordinate measured along the pipe centerline, Δx is the distance between two cross sections in the pipe, h_ℓ is the head loss, and h_s is the shaft work done by the fluid over the distance Δx. The practical application of Equation 2.53 is illustrated in Figure 2.6, where the head loss, h_ℓ, between two sections a distance Δx apart is indicated. At each cross section, the total (mechanical) energy, h, is plotted relative to a defined datum, and the locus of these points is called the *energy grade line*, commonly denoted by the acronym EGL. The EGL at each pipe cross section is located a distance $p/\gamma + \alpha V^2/2g$ vertically above the

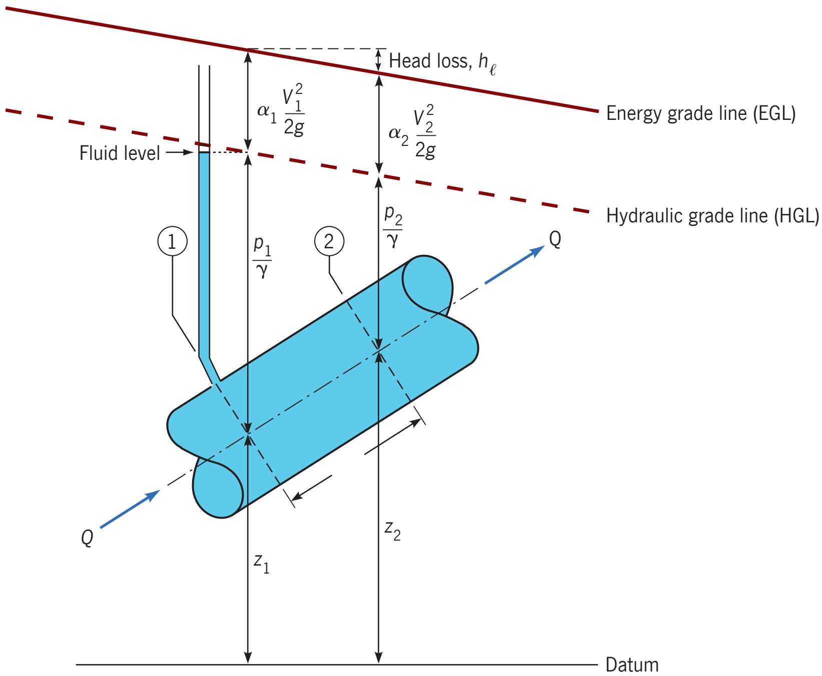

Figure 2.6: Head loss along pipe

centroid of the cross section, and between any two cross sections the elevation of the EGL falls by a vertical distance equal to the head loss, h_ℓ, plus the shaft work, h_s, done by the fluid. The *hydraulic grade line*, commonly denoted by the acronym HGL, measures the *hydraulic head*, defined as $p/\gamma + z$, at each pipe cross section. The HGL is located a distance p/γ above the centroid of the cross section, and indicates the elevation to which the fluid would rise in an open tube (piezometer) connected to the wall of the pipe section. The HGL is therefore located a distance $\alpha V^2/2g$ below the EGL. In most applications of flow in closed conduits, the velocity heads are negligible, and the HGL closely approximates the EGL. In the United Kingdom, the HGL is more commonly called the *pressure line* or the *piezometric line*.

Pump effect. Both the HGL and the EGL are useful in visualizing the state of a fluid as it flows through the pipe, and are frequently used in assessing the performance of pipeline systems. Most pipeline systems, for example, require that the fluid pressure always be positive, in which case the HGL must always be above the pipe. In circumstances where additional energy is required to maintain acceptable pressures in pipelines, a pump is installed along the pipeline to elevate the EGL by an amount h_s, which also elevates the HGL by the same amount. This condition is illustrated in Figure 2.7. In cases where the pipeline upstream and downstream of the pump have the same diameter, the velocity heads, $\alpha V^2/2g$, both upstream and downstream of the pump are the same, and the head added by the pump, h_s, goes entirely to increase the pressure head, p/γ, of the fluid. It should also be clear from Figure 2.6 that the pressure head in a pipeline can be increased by simply increasing the pipeline diameter, which reduces the velocity head, $\alpha V^2/2g$, and thereby increases the pressure head, p/γ, to maintain approximately the same total energy at the pipe section. Expansion losses will cause some reduction in the total energy.

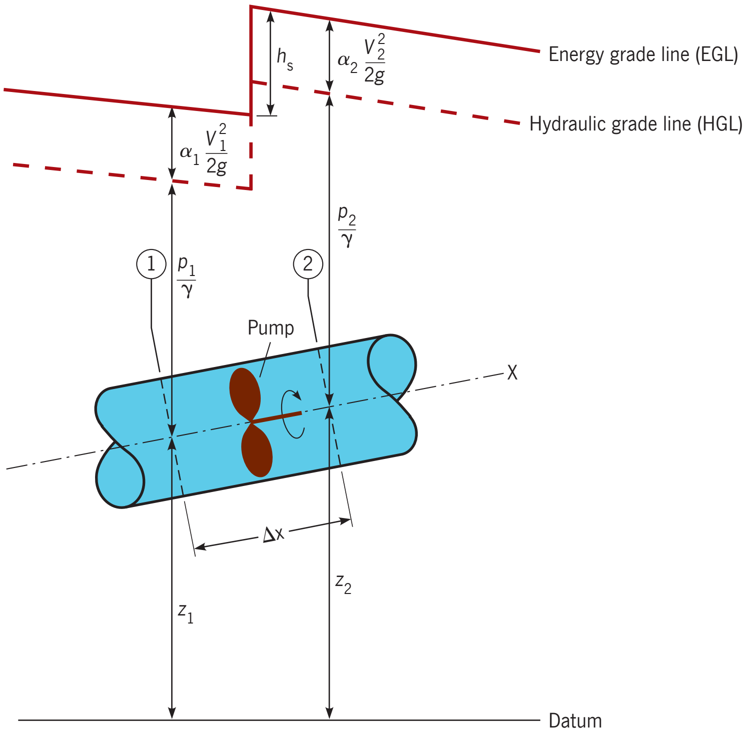

Figure 2.7: Pump effect on flow in pipeline

2.2.3.2 Velocity profile

The momentum and energy correction coefficients, α and β, at a pipe cross section both depend entirely on the velocity distribution across the section. The velocity profile in both smooth and rough pipes of circular cross section under turbulent-flow conditions can be estimated by the semi-empirical equation

$$v(r) = \left[(1 + 1.326\sqrt{f}) - 2.04\sqrt{f}\log\left(\frac{R}{R-r}\right)\right] V \tag{2.54}$$

where $v(r)$ is the velocity at a radial distance r from the centerline of the pipe, R is the radius of the pipe, f is the friction factor, and V is the average velocity across the section. The velocity distribution given by Equation 2.54 agrees well with velocity measurements in both smooth and rough pipes. This equation is not applicable within a small region close to the centerline of the pipe, and is also not applicable in a small region close to the pipe boundary. This is apparent since at the centerline of the pipe $\mathrm{d}v/\mathrm{d}r$ must be equal to zero, but Equation 2.54 does not give $\mathrm{d}v/\mathrm{d}r$ at $r = 0$. At the pipe boundary, v must be equal to zero, but Equation 2.54 gives a velocity of zero at a small distance from the wall, with a velocity of $-\infty$ at $r = R$. The energy and momentum correction coefficients, α and β, derived from the velocity profile given by Equation 2.54 are not very sensitive to the inaccuracies near the centerline and boundary, and the correction coefficients derived from Equation 2.54 are given by (Moody, 1950)

$$\alpha = 1 + 2.7f, \qquad \beta = 1 + 0.98f \tag{2.55}$$

Power-law velocity distribution. Another commonly used equation to describe the velocity distribution in turbulent pipe flow is the empirical *power law equation* given by

$$v(r) = v_0 \left(1 - \frac{r}{R}\right)^{\frac{1}{n}} \tag{2.56}$$

where v_0 is the centerline velocity. Values of n are typically in the range of 5–10, and, for any given value of f, the power-law distribution (Equation 2.56) gives the same mean velocity (V) and the same maximum (centerline) velocity (v_0) as Equation 2.54 when the following relation is satisfied

$$\left[\frac{n}{n+1} - \frac{n}{2n+1}\right] = \frac{1}{2(1+1.326\sqrt{f})} \tag{2.57}$$

The power-law distribution is not applicable within $0.04R$ of the wall, since the power-law distribution gives an infinite velocity gradient at the wall. Although the power-law distribution fits measured velocities close to the centerline of the pipe, it does not give zero slope at the centerline. The kinetic energy coefficient, α, and the momentum correction coefficient, β, derived from the power-law distribution are given by

$$\alpha = \frac{(n+1)^3(2n+1)^3}{4n^4(n+3)(2n+3)}, \qquad \beta = \frac{(n+1)^2(2n+1)^2}{2n^2(n+2)(2n+2)} \tag{2.58}$$

For n values in the range of 5–10, corresponding values of α are in the range of 1.11–1.03, and values of β are in the range of 1.04–1.01. In most engineering applications, it is assumed that $\alpha = 1$ and $\beta = 1$; errors introduced by these assumptions are usually negligible.

Velocity distribution in laminar flow. The above results are applicable only for turbulent flow in pipes, which is the most frequently encountered pipe-flow condition in hydraulic engineering. In cases of laminar flow, the velocity distribution is given by

$$v(r) = v_0 \left(1 - \frac{r^2}{R^2}\right) \tag{2.59}$$

which yields $\alpha = 2$ and $\beta = \frac{4}{3}$. Hence, under laminar flow conditions, the approximations that $\alpha = 1$ and $\beta = 1$ might not be appropriate.

Example 2.6
Water at 20°C flows through a 300-mm diameter pipe at a rate of 150 L/s, and the equivalent sand roughness of the pipe is 0.5 mm. (a) Compare the velocity distributions given by Equations 2.54 and 2.56 based on matching the maximum velocity and using an n value given by Equation 2.57. (b) Compare the energy and momentum correction coefficients for each of the velocity distributions considered in Part (a), and assess the common assumption that these factors can be taken as approximately equal to unity.

Solution.
From the given data: D = 300 mm = 0.3 m, Q = 150 L/s = 0.15 m^3/s, and k_s = 0.5 mm. For water at 20°C, $\nu = 1.00\times10^{-6}$ m^2/s. The following preliminary calculations are useful:

$$A = \frac{\pi D^2}{4} = \frac{\pi(0.3)^2}{4} = 7.069\times10^{-2}\ \text{m}^2, \qquad V = \frac{Q}{A} = \frac{0.15}{7.069\times10^{-2}} = 2.122\ \text{m/s}$$

$$\text{Re} = \frac{VD}{\upsilon} = \frac{(2.122)(0.3)}{1.00\times10^{-6}} = 6.366\times10^{5}, \qquad \frac{k_s}{D} = \frac{0.5}{300} = 1.667\times10^{-3}$$

The friction factor, f, can be determined by substituting Re and k_s/D into the Colebrook equation (Equation 2.28) which gives

$$\frac{1}{\sqrt{f}} = -2\log\left[\frac{k_s/D}{3.7} + \frac{2.51}{\text{Re}\sqrt{f}}\right] \quad\rightarrow\quad \frac{1}{\sqrt{f}} = -2\log\left[\frac{1.667\times10^{-3}}{3.7} + \frac{2.51}{6.366\times10^{5}\sqrt{f}}\right] \quad\rightarrow\quad f = 0.0227$$

(a) The centerline velocity, v_0, given by the logarithmic velocity profile (Equation 2.54) occurs at $r = 0$; therefore,

$$v_0 = \left[(1+1.326\sqrt{f}) - 2.04\sqrt{f}\log\left(\frac{R}{R-0}\right)\right]V \quad\rightarrow\quad v_0 = (1+1.326\sqrt{f})V$$

where V is the average velocity. Normalizing the logarithmic velocity distribution by v_0, and using the calculated value for f, gives

$$\frac{v}{v_0} = 1 - \frac{2.04\sqrt{f}}{1+1.326\sqrt{f}}\log\left[\frac{1}{1-(r/R)}\right] \quad\rightarrow\quad \frac{v}{v_0} = 1 - 0.265\log\left[\frac{1}{1-(r/R)}\right] \tag{2.60}$$

Considering the power-law velocity distribution, the exponent, n, as given by Equation 2.57 is

$$\left[\frac{n}{n+1} - \frac{n}{2n+1}\right] = \frac{1}{2(1+1.326\sqrt{0.0227})} \quad\rightarrow\quad n = 7.84$$

and hence the normalized power-law velocity distribution given by Equation 2.56 can be expressed as

$$\frac{v}{v_0} = \left(1-\frac{r}{R}\right)^{\frac{1}{n}} \quad\rightarrow\quad \frac{v}{v_0} = \left(1-\frac{r}{R}\right)^{0.128} \tag{2.61}$$

The logarithmic and power-law velocity distributions are plotted and compared in Figure 2.8.

It is apparent from Figure 2.8 that the logarithmic and power-law velocity distributions are in very close agreement, and the "full" velocity profile that is characteristic of turbulent flows is apparent. However, the discrepancy that the velocity gradient does not asymptote to zero at the centerline of the pipe gives a sense of unreality to the computed velocity distribution near the centerline.

(b) The energy and momentum correction coefficients corresponding to the logarithmic velocity distribution are given by Equation 2.55, which yield

$$\alpha = 1 + 2.7f = 1 + 2.7(0.0227) = 1.06, \qquad \beta = 1 + 0.98f = 1 + 0.98(0.0227) = 1.02$$

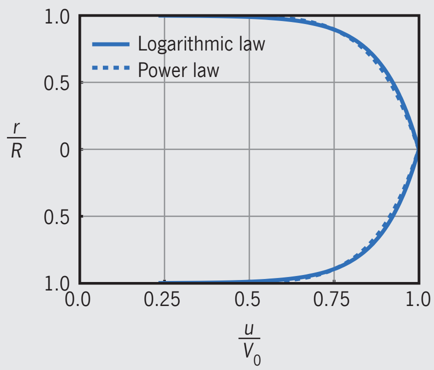

Figure 2.8: Comparison of turbulent velocity distributions

The energy and momentum factors corresponding to the power-law velocity distribution are given by Equation 2.58, which yield

$$\alpha = \frac{(n+1)^3(2n+1)^3}{4n^4(n+3)(2n+3)} = \frac{(7.84+1)^3[2(7.84)+1]^3}{4(7.84)^4(7.84+3)[2(7.84)+3]} = 1.05$$

$$\beta = \frac{(n+1)^2(2n+1)^2}{2n^2(n+2)(2n+2)} = \frac{(7.84+1)^2[2(7.84)+1]^2}{2(7.84)^2(7.84+2)[2(7.84)+2]} = 1.02$$

Comparing the derived values of α and β for the logarithmic and power-law velocity distributions shows that, with the retention of three significant digits, the values of α differ by 0.01, and the values of β are the same. For this case, **the common assumption that $\alpha \approx 1$ and $\beta \approx 1$ seems reasonable**.

2.2.3.3 Local head losses

Head losses in straight pipes of constant diameter are caused by friction between the moving fluid and the stationary pipe boundary, and are estimated using the Darcy–Weisbach equation. Flow through pipe fittings, around bends, and through changes in pipeline geometry cause additional head losses that are typically quantified by an equation of the form

$$h_{\text{local}} = K\frac{V^2}{2g} \tag{2.62}$$

where h_{local} is the local head loss, K is a *local-loss coefficient*, and V is the average velocity at a defined location within the transition or fitting. The head-loss coefficient, K, is a function of both the geometry of the fitting and a characteristic Reynolds number (Re) of the flow through the fitting. However, Re is usually sufficiently high that viscous effects are negligible, in which case K can be taken to be a function of the geometry of the fitting only. If the inflow and outflow sections of a fitting have the same cross-sectional area and elevation, then the steady-state energy equation requires that

$$h_{\text{local}} = -\frac{\Delta p}{\gamma} \tag{2.63}$$

where Δp is the difference between the outflow pressure and the inflow pressure, and γ is the specific weight of the fluid. Combining Equations 2.62 and 2.63 gives the following useful relation between the head-loss coefficient and the pressure change across a fitting:

$$K = -\frac{\Delta p}{\frac{1}{2}\rho V^2} \tag{2.64}$$

The pressure will generally decrease across a fitting, so values of Δp will generally be negative. In applications involving head-loss coefficients, Equation 2.62 is the relation that is most commonly used in calculating local head losses. Head losses in transitions and fittings are called *local head losses* or *minor head losses*; however, the latter term should be avoided since in some cases these head losses are a major portion of the total head loss in a conduit. Commonly encountered transitions include bends, tees, and changes in diameter; while commonly encountered fittings include various types of valves, such as gate valves that are used to open and close pipelines carrying liquids, and globe valves that are used to regulate the flow of liquids in pipelines and are used as faucets at the end of pipes in household plumbing. The loss coefficients for several transitions and fittings are shown in Figures 2.9 and 2.10, where the locations of the velocities to be used in Equation 2.62 to calculate the local head loss are also shown.

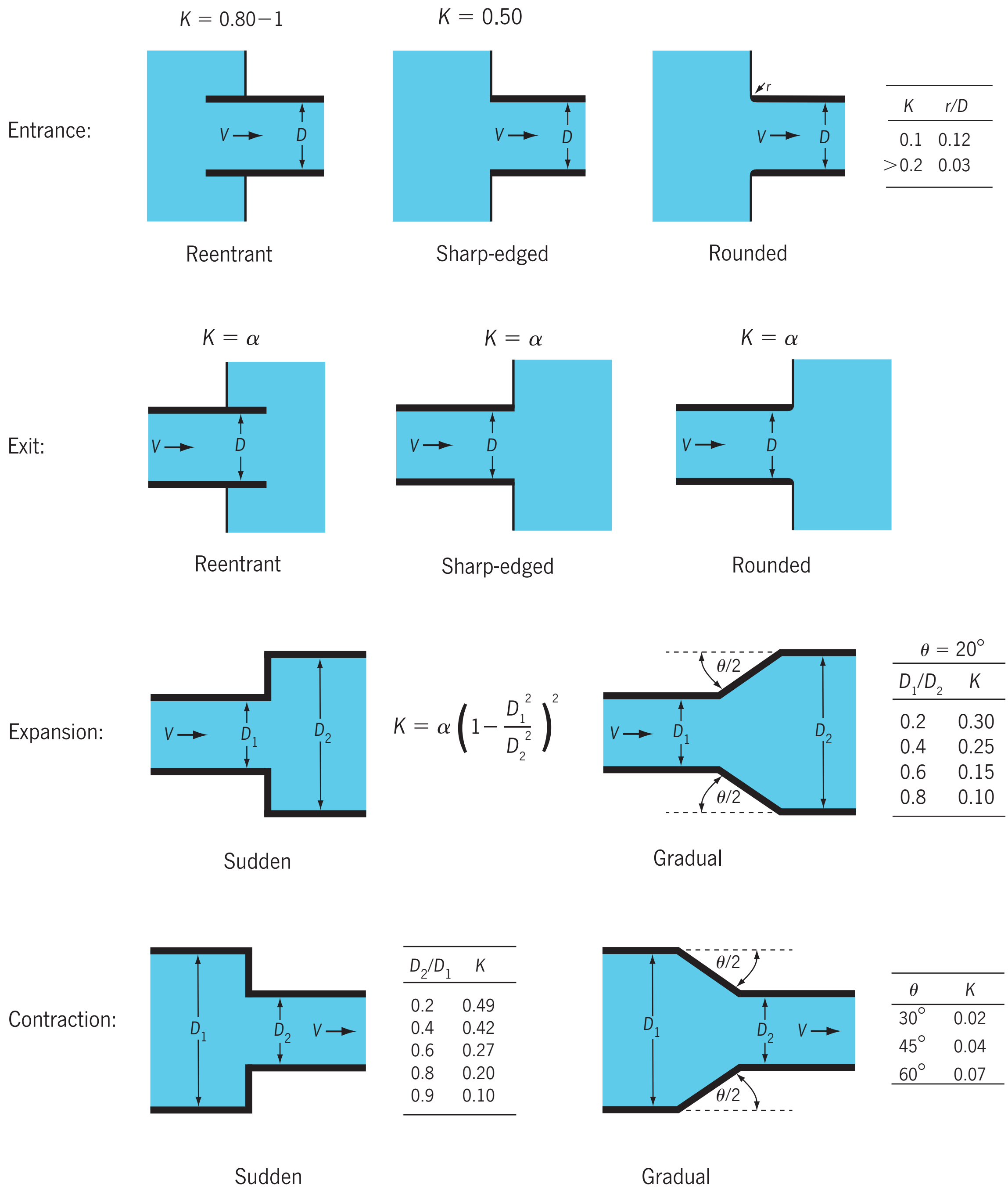

Figure 2.9: Loss coefficients for entrances, exits, expansions, and contractions

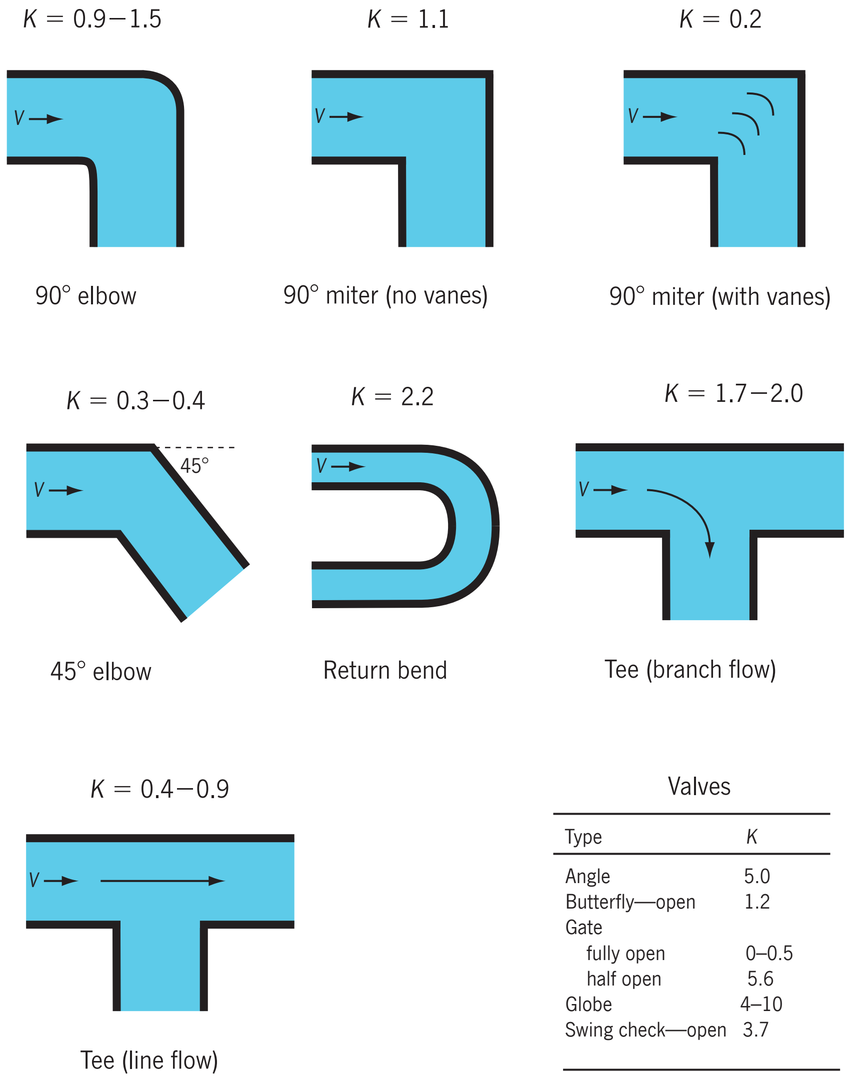

Valves

Type	K
Angle	5.0
Butterfly—open	1.2
Gate	
fully open	0–0.5
half open	5.6
Globe	4–10
Swing check—open	3.7

Figure 2.10: Loss coefficients for bends, tees, and valves

General guidelines. There is considerable uncertainty in the local-loss coefficients given in Figures 2.9 and 2.10, since local-loss coefficients generally vary with surface roughness, Reynolds number, and the geometric details. The loss coefficients of two seemingly identical valves from two different manufacturers can differ by a factor of 2 or more. Also, whether a fitting is screw-connected or flange-connected can significantly affect the head-loss coefficient of the fitting. In cases of identical fitting geometry, with the only difference being a screw connection versus a flange connection, the fitting with the screw connection will typically have a significantly higher head-loss coefficient. However, differences in the geometry of the fitting itself can mask differences in the type of connection. For purposes of brevity, the ranges of loss coefficients given in Figures 2.9 and 2.10 include both screw and flange connections, and also reflect the range of unit designs and materials that are used in various transitions and fittings. Based on these considerations, recent and fitting-specific manufacturer's data should be consulted in the final design of piping systems, rather than relying on the representative values in textbooks and handbooks.

Head losses at inlets and outlets. Head losses at submerged pipe inlets are significantly influenced by the geometry of the inlet, with the head-loss coefficient, K, varying from 0.03 for a well-rounded inlet to 0.80 for a reentrant (i.e., protruding) inlet. It is apparent that minimization of inlet losses can be achieved by rounding inlets. At submerged outlets, pipe flows typically lose all of their velocity head, and so K at a submerged pipe outlet is equal to the kinetic-energy correction coefficient, α, regardless of the geometry of the outlet. For fully developed turbulent flows in pipes, $\alpha \approx 1$ and so $K = 1$ is widely used to estimate the head loss at a submerged outlet. However, recognizing that $\alpha = 2$ for fully developed laminar flow in pipes, it is prudent to use the general relation $K = \alpha$ in calculating local head losses at submerged outlets. Since the head loss at a submerged outlet is independent of the outlet geometry, there is no advantage to rounding sharp edges in pipe outlets.

Head losses in expansions and contractions. Within pipeline systems, changes in diameter can occur either suddenly or gradually within a fitting, with a greater head loss occurring for a sudden change in diameter compared to a gradual change. For both expansions and contractions, the velocity in the smaller pipe is used in Equation 2.62 to calculate the local head loss, and losses in expansions are typically much higher than losses in comparable contractions, primarily due to the flow separation that occurs in expansions. The local-loss coefficient in a sudden contraction, K_{sc}, can be estimated by

$$K_{sc} = \begin{cases} 0.42\left(1 - \dfrac{D_2^2}{D_1^2}\right), & \text{for } D_2/D_1 \leq 0.76 \\ \left(1 - \dfrac{D_2^2}{D_1^2}\right)^2, & \text{for } D_2/D_1 > 0.76 \end{cases} \tag{2.65}$$

where D_1 and D_2 are the upstream and downstream diameters, respectively. The local-loss coefficient in a sudden expansion, K_{se}, can be estimated by

$$K_{se} = \left(1 - \frac{D_1^2}{D_2^2}\right)^2 \tag{2.66}$$

where D_1 and D_2 are the upstream and downstream diameters, respectively. Equation 2.66 can be derived theoretically (e.g., Massey and Ward-Smith, 2012), and the head loss calculated using this coefficient is sometimes called the *Borda-Carnot head loss*[†]. A gradual expansion is commonly called a *diffuser*, a term that is sometimes generically used to refer to an expanding conduit. Head losses due to flow separation are of particular concern in the design of diffusers, and such losses can be controlled by proper selection of the expansion angle, θ, illustrated in Figure 2.9. The local-loss coefficient, K_{ge}, in a diffuser or gradual expansion can be estimated by the relation (White, 2011)

$$K_{ge} = 2.61 \sin\left(\frac{\theta}{2}\right)\left(1 - \frac{D_1^2}{D_2^2}\right)^2 + \frac{f_{ge}L_{ge}}{\overline{D}_{ge}}, \quad \text{for } \theta \leq 45^\circ \tag{2.67}$$

[†]Named after J.-C. Borda (1733–1799) and L.M.N. Carnot (1753–1823).